JOURNAL OF NEUROTRAUMA 38:1551–1571 (June 1, 2021)

DOI: 10.1089/neu.2020.7254

Original Article

Behavioral and Myelin-Related Abnormalities after Blast-Induced Mild Traumatic Brain Injury in Mice

Mio Nonaka,[1] William W. Taylor,[1] Olena Bukalo,[1] Laura B. Tucker,[2,3] Amanda H. Fu,[2,3] Yeonho Kim,[2,3] Joseph T. McCabe,[2,3] and Andrew Holmes[1]

Abstract

In civilian and military settings, mild traumatic brain injury (mTBI) is a common consequence of impacts to the head, sudden blows to the body, and exposure to high-energy atmospheric shockwaves from blast. In some cases, mTBI from blast exposure results in long-term emotional and cognitive deficits and an elevated risk for certain neuropsychiatric diseases. Here, we tested the effects of mTBI on various forms of auditory-cued fear learning and other measures of cognition in male C57BL/6J mice after single or repeated blast exposure (blast TBI; bTBI). bTBI produced an abnormality in the temporal organization of cue-induced freezing behavior in a conditioned trace fear test. Spatial working memory, evaluated by the Y-maze task performance, was also deleteriously affected by bTBI. Reverse-transcription quantitative real-time polymerase chain reaction (RT-qPCR) analysis for glial markers indicated an alteration in the expression of myelin-related genes in the hippocampus and corpus callosum 1–8 weeks after bTBI. Immunohistochemical and ultrastructural analyses detected bTBI-related myelin and axonal damage in the hippocampus and corpus callosum. Together, these data suggest a possible link between blast-induced mTBI, myelin/axonal injury, and cognitive dysfunction.

Keywords: blast; fear learning; mTBI; myelin; nodes of Ranvier

Introduction

Traumatic brain injuries (TBIs) affect 1.7 million people in the United States and 69 million persons worldwide.[1,2] Mild TBI (mTBI) is the most prevalent form, and its long-term effects are a significant healthcare concern. Among the causes of mTBI, exposure to an intense shockwave from an improvised explosive device in a combat arena has been shown to have deleterious effects on neurocognitive performance.[3–5] In military settings, a significant proportion (10–20%, or nearly 200,000) of returning soldiers from the wars in Iraq and Afghanistan had reportedly sustained one or more blast exposures.[6–8] In accidents and terrorist attacks civilians are also at risk from blast-related injury, and, unlike military personnel, risk is not mitigated by protective clothing that shields against blast impact.[9,10]

The physical impact of blast can differ from other forms of mTBI by exposure to overpressure and intense energy, as an additional sources of injury.[11,12] Clinically, primary blast injury often presents with secondary (physical damage from blast fragments) and tertiary effects (TBIs by impact collisions), as well as other physical injuries. However, it is important to delineate the consequences of the primary blast injury. Animal models are valuable in this regard by enabling the study of the effects of blast exposure *per se*.[13,14] To this end, procedures have been developed that use shock tubes to simulate blast TBI (bTBI) in rats and mice, where the primary injurious force is caused by atmospheric overpressure from highly controlled blast waves generated within compressed air-driven shock tubes.[12,15–20]

In pre-clinical bTBI models, injury-related impairments have been reported for measures of cognition (e.g., active avoidance response, operant learning task, and Morris water maze),[21–23] as well as tests for fear- and anxiety-related behavior.[24–26] These findings are particularly pertinent given clinical evidence of cognitive deficits in persons with blast exposure history[6,27,28] and the high comorbidity of TBI with trauma and stressor-related disorders (formerly post-traumatic stress disorder).[29–31] However, the neural basis of these behavioral sequelae of bTBI remains unclear, though several studies of blast-exposed personnel suggest that bTBI damages cerebral white matter.[32–38] The aim of the current study was to assess the consequences of single and repeated bTBI on various measures of cognitive function in mice (delay fear conditioning and extinction, trace fear conditioning, social recognition, and spatial working memory) and test for associated changes in myelination, by convergent structural, gene expression, and protein expression analyses.

[1]Laboratory of Behavioral and Genomic Neuroscience, National Institute on Alcohol Abuse and Alcoholism, National Institutes of Health (NIH), Rockville, Maryland, USA.
[2]Department of Anatomy, Physiology and Genetics, [3]Preclinical Studies Core, Center for Neuroscience and Regenerative Medicine, Uniformed Services University of the Health Sciences, Bethesda, Maryland, USA.

Table 1. Summary of Tests Performed for the Various Experimental Cohorts

Mouse cohort	*Blast*	*Procedure 1*	*Procedure 2*	*Procedure 3*	*Procedure 4*	*Procedure 5*	*Procedure 6*
Cohort 1	1×Sham/1×Blast	Delay fear Cond/Ext/Ret/Ren test (1 week)	RT-qPCR (1 week)				
Cohort 2	1×Sham/1×Blast	Delay fear Cond/Ext/Ret/Ren test (2 weeks)	RT-qPCR (2 weeks)				
Cohort 3	1×Sham/1×Blast	Delay fear Cond/Ext/Ret/Ren test (4 weeks)	RT-qPCR (4 weeks)				
Cohort 4	1×Sham/1×Blast	Delay fear Cond/Ext/Ret/Ren test (8 weeks)	RT-qPCR (8 weeks)				
Cohorts 6 and 8	4×Sham/4×Blast	Delay fear Cond/Ext/Ret/Ren test (3 days)					
Cohorts 7, 9, and 12	4×Sham/4×Blast	Delay fear Cond/Ext/Ret/Ren test (2 weeks)					
Cohorts 5, 10, and 11	4×Sham/4×Blast	Delay fear Cond/Ext/Ret/Ren test (8 weeks)					
Cohort 13	4×Sham/4×Blast	Trace fear cond test (3 days)	Trace fear cond test (3 days)				
Cohort 14	1×Sham/1×Blast	Y-maze (3 days)	Social recog (3 days)	Trace fear cond test (1 week)	Nodes of Ranvier staining (1 week)	CNP staining (1 week)	
Cohort 15	1×Sham/1×Blast	Y-maze (8 weeks)	Social recog (8 weeks)	Trace fear cond test (8 weeks)	Nodes of Ranvier staining (8 weeks)	CNP staining (8 weeks)	
Cohorts 16 and 17	4×Sham/4×Blast	Y-maze (3 days)	Social recog (3 days)	Trace fear cond test (1 week)	Nodes of Ranvier staining (1 week)	CNP staining (1 week)	EM analysis (1 week) for some animals
Cohort 18	4×Sham/4×Blast	Social recog (8 weeks)	Trace fear cond test (8 weeks)	CNP staining (8 weeks)			
Cohort 19	1×Sham/1×Blast	Trace fear cond test (3 days)					
Cohort 20	1 and 3 1×Sham/1×Blast	MBP staining and Black Gold II (1 week)					
Cohort 21	2 and 4 1×Sham/1×Blast	MBP staining and Black Gold II (2 weeks)					

Some cohorts were used for multiple behavioral assays and biochemical or histological assays. Time shown in parentheses indicates the timing of the behavior tests performed or the animals euthanized for later histological or biochemical assays.

CNP, 2′,3-cyclic nucleotide-3-phosphodiesterase; EM, electron microscopy; MBP, myelin basic protein; RT-qPCR, reverse-transcription quantitative real-time polymerase chain reaction.

Methods

Subjects

Male C57BL/6J mice (8–9 weeks of age at the time of blast) were obtained from the Jackson Laboratory (Cat No. 000664; Bar Harbor, ME), singly housed in a temperature- and humidity-controlled vivarium under a 12-h light/dark cycle (lights on 6:00 AM), and acclimated for at least 1 week before the commencement of blast procedures. Food and water were available *ad libitum*. After blast exposure, mice remained in the animal facility overnight before being transported (~9.3 km) in their home cages from the Uniformed Services University to the Laboratory of Behavioral and Genomic Neuroscience, National Institute on Alcohol Abuse and Alcoholism (NIAAA). After a minimum 3-day acclimation at the NIAAA, behavior experiments were performed by researchers who were blind to the blast/sham conditions. For logistical reasons, multiple cohorts were separately tested to generate the full sample—with mice from the bTBI and sham conditions always represented within a cohort. The sequence of experimental procedures is summarized in Table 1.

Experimental procedures were performed in accordance with the National Institutes of Health Guide for Care and Use of Laboratory Animals and approved by the local NIAAA and Uniformed Services University of the Health Sciences (USUHS) Animal Care and Use committees. The initial number of mice generated in each experiment was 58 mice that received Sham (1×) treatment, 57 mice that received 1×Blast, 72 mice that received Sham (4×) treatment, and 115 mice that were assigned to the 4×Blast treatment. The number of animals used in the final analysis, after exclusions attributable to death after blast, is indicated in the figure legends.

Blast injury

Blast exposures were performed at the USUHS site with an Advanced Blast Simulator (ABS[39]) as described previously.[15,40] The driver section of the ABS was separated from the transition section with two or three acetate sheets (0.254-mm thickness each; Grafix Plastics, Cleveland, OH) and two vinyl-mesh layers (mesh size 14.5×10 grids/in^2, wire diameter 0.635 mm, Pet Screen, Hanover/New York Wire, Cat. No. 70589). The driver was sealed by the membrane material and pressurized to 150–160 psi, before bursting the acetate/vinyl membrane. For single shock-wave exposure (1×Blast, ~15 psi peak pressure, recorded from a pencil gauge positioned adjacent to the animal), mice were anesthetized with 3% isoflurane in 100% oxygen for 4–6 min and placed in a mesh rodent holder, with their ventral side facing the blast source. For repeated blast (4×Blast, ~15 psi peak pressure), mice were subjected to the blast procedure once per day for four consecutive days. Sham controls underwent the same procedures as the relevant single and repeated blast group (1×or 4×Sham), with the exception that no shockwave was delivered.

Delay cued fear conditioning and extinction

Delay fear conditioning was conducted essentially as previously described.[41–43] Conditioning was conducted in a 30×25×25 cm chamber with metal walls and a metal rod floor (Context A). To provide an olfactory cue, the context was cleaned between subjects with a 79.5% water/19.5% ethanol/1% vanilla extract solution. After a 180-sec acclimation period, the mouse received three pairings of a 20 sec, 70-dB white noise cue (conditioned stimulus; CS), that coterminated with a 2 sec, 0.6-mA scrambled footshock (unconditioned stimulus; US). Pairings were separated by a variable 60- to 90-sec interpairing interval. Mice remained in the testing context for 60 sec after the final pairing.

Fear extinction was performed the next day in a novel context, Context B: a 27×27×11 cm chamber with curved white Plexiglas walls and a floor of the same material, cleaned with a 99% water/1% acetic acid solution and located in a different room from Context A. After a 180-sec baseline, mice received 50×CS presentations with a 5-sec inter-CS interval. The next day, extinction retrieval was tested in Context B: 5×CS presentations (5 sec of intertrial interval) after a 180-sec baseline. Later that day, fear renewal was tested by repeating the retrieval procedure, but with 3×CS presentations in Context A. CS and US presentations were controlled by the Med Associates Freeze Monitor System (Med Associates, Fairfax, VT). Freezing, as an index of fear, was scored manually by a researcher blind to blast group. Freezing was defined as the absence of any visible movement, except that required for

respiration, and was scored at 5-sec intervals by an observer blind to genotype. The number of observations scored as freezing was converted to a percentage, [(number of freezing observations/total number of observations) × 100], for analysis.

Trace fear conditioning

Trace fear was tested essentially as previously described.[44,45] Conditioning was conducted in a 30 × 25 × 25 cm chamber with metal walls and a metal rod floor (Context A). After a 180-sec acclimation period, the mouse received three pairings of a 20-sec, 70-dB white noise CS, followed by a 20-sec trace period and then a 2-sec, 0.6-mA scrambled footshock US. Pairings were separated by a variable 150- to 270-sec pairing interval. Mice remained in the testing context for 60 sec after the final pairing.

To evaluate fear retrieval, responses to the CS were assessed on the second day in a novel context (Context B). After a 300-sec baseline period, mice received five CS presentations, separated by a 20-sec interval (Trace). On the third day, mice were placed in Context A, where they had received fear conditioning, for 300 sec to evaluate context memory retrieval. Freezing episodes, >1 sec in duration, were scored automatically by Video Freeze software (Med Associates), and percentage of freezing time in defined behavioral test phases (baseline, CS, and trace) was calculated.

Social recognition test

Social recognition was tested as described previously.[46] In brief, the test mouse was placed in a novel home cage (14 × 36 cm), lined with fresh corn cob bedding, under dim light (21 lux). After a 15-min habituation period, an unfamiliar juvenile (post-natal day 45) mouse was placed in the cage for a 2-min sample period, and then both mice were returned to their home cages. Thirty minutes later, both mice were returned to the testing environment for a 2-min test period. Behavior was recorded using a GoPro HERO5 Black camera (GoPro Inc., San Mateo, CA). Social interaction was manually scored by a researcher blind to the blast exposure condition, as the summed duration of test mouse sniffing, following, or otherwise attending (within 1 cm) to the juvenile mouse.[46] The difference in social interaction time (*sample-test*) and the proportional change in interaction time (*test/sample*) was calculated.

Spatial novelty preference Y-maze test

The Y-maze test was based on a previously described procedure.[47] The apparatus consisted of three 30-cm-long arms, with 20-cm-high walls, constructed of clear acrylic, positioned at a 120-degree angle to one another and located in a room with handmade three-dimensional distal spatial cues. The floor of the maze was covered with a mixture of clean and dirty (from an unfamiliar, male mouse) bedding, at a ratio of 3:1. Arms were designated (spatial location counterbalanced across mice) as home, familiar, or novel. During the sample trial, the novel arm was blocked. Mice were individually placed at the end of the home arm, facing away from the familiar and novel arms, and after 5-min, they were returned to the home cage. One minute later, the mouse was returned to the maze, with the novel arm freely accessible and the bedding redistributed throughout the apparatus, for a 2-min test period. Behavior was recorded using a GoPro HERO5 Black camera.

The number of arm entries and total duration in the familiar and novel arms in the first minute of the test period was manually scored by a researcher blinded to the blast exposure condition and calculated to generate measures of novel arm preference as 1) *Preference Index (duration) = time in novel arm/(time in novel arm + time in familiar arm)* and 2) *Preference Index (entries) = #entries into novel arm/(#entries into novel arm + #entries into familiar arm)*. An entrance into the arms was scored when the mouse had all four paws in the arm.

RNA purification and reverse-transcription quantitative real-time polymerase chain reaction

A subset of mice from 1 × Sham and 1 × Blast were euthanized by cervical dislocation 2 days after completing fear and extinction testing (see Table 1). The head was briefly chilled in ice-cold PBS and the brain extracted on ice and flash-frozen in dry, ice-cold 2-methylbutane. Brain regions of interest (ROIs) were punched and transferred to RNAlater (Qiagen, Hilden, Germany). RNA was extracted using the Qiagen RNeasy Lipid Tissue Mini kit (Qiagen). Fifty nanograms of RNA was used to synthesize complementary DNA (cDNA) using reverse transcriptase (iScript; Bio-Rad Laboratories, Hercules, CA), and one twenty-fifth of its volume was used for the RT-qPCR reaction to quantify the cDNA of interest. RT-qPCR was performed using Power SYBR Green PCR Master Mix (Applied Biosystems, Foster City, CA) with a StepOnePlus Real-Time qPCR instrument (Applied Biosystems). PCR was performed as follows: 1 × denature (95°C for 20 sec) and 46 × PCR (95°C for 3 sec, 60°C for 30 sec), and relative mRNA levels were determined by normalizing cycle threshold (Ct) values of the target and reference housekeeping gene, glyceraldehyde 3-phosphate dehydrogenase (*Gapdh*), using the ΔΔCt method. Primers were designed by primerBLAST (NIH, Bethesda, MD), and the sequences are provided in Table 2.

Table 2. Summary of the Primers Used in RT-qPCR

Gene	*Forward (5′ - 3′)*	*Reverse (5′ - 3′)*	*Amplicon size*	*Amplicon location*
Gfap	TGGCCACCAGTAACATGCAA	CTCTAGGGACTCGTTCGTGC	188 bp	coding region (Rev primer spanning exon)
Aqp4	TTCTCTTCGGTGCTAGGAAAC	AGGAAGCTTATGTCTCTGGTG	158 bp	3′ UTR
Mbp	CAGAAGAGACCCTCACAGCG	CTAAAGAAGCGCCCGATGGA	125 bp	coding region
Gpr17	TGGCTGTTACCCCACTTGTC	TCTTCTGTGGCCCCCATTTG	147 bp	3′ UTR
Olig2	TTACAGACCGAGCCAACACC	TGGCCCCAGGGATGATCTAA	129 bp	5′ UTR and start codon
Nefh	ACCACCAGGAGGAGGTGG	GTCCAACCTCACTCGGAACC	197 bp	coding region (exon spanning)
Hapln2	CCTGAAGCAGCCAGACATCC	ACTCCCTAGTACTGCAAGATGA	156 bp	5′ UTR (exon spanning)
Agrin	CCTACTCCTGCAAGGTTCGAG	GACACCTGGTTGTCGCAGAT	136 bp	coding (exon spanning)
Vcan	ACCCGAGACCTACCCTGAAA	ACAGAGGGACAGGCTTAGGT	170 bp	coding region
CNPase	CAGCAGGAGGTGGTGAAGAG	AGATCACTGGGCCACAACTG	134 bp	coding region
Ng2 (Cspg4)	CCAGGTGCTGTTCAGCGTGAG	CATCAGCTGGTCAGAGGTGTC	160 bp	coding region
TN-R	CGTGAAGCCTTCTCTCTGCC	AGTTGATGCAGACACCCAGG	184 bp	5′ UTR (exon spanning)
Gapdh	AATGCATCCTGCACCACCAAC	TGGATGCAGGGATGATGTTCTG	187 bp	coding region

Primer sequences and properties of a pair of primers per gene are listed. All primers produced amplicons of a single peak in the melting curve analysis performed at the end of the RT-qPCR reaction.

RT-qPCR, reverse-transcription quantitative real-time polymerase chain reaction; UTR, untranslated region.

Immunohistochemistry and immunostaining

A subset of mice (most of the mice that were not used for PCR) were deeply anesthetized with sodium pentobarbital and transcardially perfused with 4% paraformaldehyde in phosphate-buffered saline (PBS). Brains were removed and post-fixed overnight. The next day, brains were transferred to a 15% sucrose PBS solution and then to a 30% sucrose in PBS solution. After sinking in the 30% sucrose/PBS, brains were frozen with dry ice-cold 2-methylbutane and stored at −80°C until they were sectioned on a CM 3050S (Leica Biosystems, Wetzler, Germany), or a Microm HM500 OM (ThermoFisherScientific, Waltham, MA), cryostat.

For 2′,3-cyclic nucleotide-3-phosphodiesterase (CNPase) and myelin basic protein (MBP) immunostaining, 50-μm coronal sections were washed in PBS, blocked with 1% BSA, 10% normal goat serum, and 0.3% Triton-X 100 in PBS for 2 h at room temperature, then incubated for 2 overnights on a shaker at 4°C with antibodies against CNPase (D83E10, rabbit monoclonal immunoglobulin G [IgG], 1:100; Cell Signaling Technology, Danvers, MA), MBP (SMI-99 mouse monoclonal IgG, 1:1000; Millipore Sigma, Burlington, MA), or glial fibrillary acidic protein (GFAP; rabbit polyclonal IgG, 1:2500; DAKO/Agilent Technologies, Santa Clara, CA). Images were acquired using a Zeiss LSM 700 laser scanning confocal microscope with an EC Plan-NEOFLUAR 10×/0.30 objective. To ensure that the same level of optical sections was taken across all the samples, we obtained three z-stack images from the tissue attached to the cover-slip surface and used only the middle plane for analysis. Details of fluorescent signal quantification are described in the *Analysis of myelin density* section below.

For Black Gold II (Millipore Sigma) staining, 30-μm-thick coronal sections were mounted directly on gelatinized slides. Sections were washed in deionized H_2O for 2 min and stained in Black Gold II for 12 min, then washed twice in DI H_2O and submerged in a sodium thiosulfate solution for 3 min. Sections were washed another three times before being stained in cresyl violet (Millipore Sigma) for 3 min and then washed another three times. Finally, sections were dehydrated in a graded alcohol series (70%-95%-95%-100%-100%), two xylene washes, and cover-slipped using Permount (ThermoFisherScientific).

For staining the nodes of Ranvier, 18-μm-thick coronal sections were cut and directly mounted on slides. Slides were washed with PBS and blocked with 5% goat serum, 0.5% BSA, and 0.5% Triton-X-100, in PBS and incubated for 48 h at 4°C in a humidified slide chamber with anti-Nav1.6 antibody (rabbit polyclonal IgG, 1:200; Alomone Labs Ltd., Jerusalem, Israel [as previously described[48]]) and anti-Caspr antibody (K65/35 mouse monoclonal IgG_1, 1:100; NeuroMab, Davis, CA). Images were acquired with a Zeiss LSM 880, using a Plan-Apochromat 63×/1.40 Oil DIC objective (Carl Zeiss, Jena, Germany).

Measurement of nodes of Ranvier

Under the microscope, coronal sections (bregma +0.4 to +0.5) were selected with reference to the mouse brain atlas,[49] and the corpus callosum area close to the midline (between the lateral ventricles) was set as the acquisition area. Three optical sections were taken at 0.44-μm intervals and projected as single planes for length analysis. For each mouse, 30 nodes of Ranvier were randomly selected and the length of the nodal gap was measured using NIH ImageJ software[50] by a researcher blind to the blast exposure condition.

Analysis of myelin density

Myelin density was determined using a custom-written Matlab code (Matlab 2018a; The MathWorks, Inc., Natick, MA) with an image-processing toolbox. Two lines, 200 μm apart, spanning the full layers of the CA1 area of the hippocampus, were drawn onto the Hoechst channel of the MBP- or CNPase-stained images of the CA1. Intensity profile of the fluorescent pixel intensity signal (16-bit), average of mediolateral axis, was created along the dotted lines. Averaged values from different images were aligned for the dorsoventral level by using the peak of Hoechst signal intensity in the pyramidal cell layer, and the same ROI (the area defined by two lines) was applied for the immunostained channels of the same images. Then, intensity profiles of Hoechst fluorescent signal, MBP immunofluorescent signal, or CNPase immunofluorescent signal, along the dorsoventral axis of CA1, were graphed. To detect the most affected layer of hippocampal CA1, MBP signal intensity was normalized to the min/max value of each ROI of the image by this equation, Normalized intensity = [Intensity − min(intensity) / Max(Intensity) − min(Intensity)], and plotted. For Black Gold II staining of myelin, the brightfield image was processed for color deconvolution to split Nissl staining and Black Gold II signals using Fiji software, and the Black Gold II signal in *stratum oriens* of the CA1 area of the hippocampus was quantified.

Electron microscopy

A subset of mice (1 mouse from each of the 4×Sham and 4×Blast groups at the 1- and 8-week post-blast intervals) were deeply anesthetized with sodium pentobarbital and transcardially perfused with 2.5% glutaraldehyde and 2% paraformaldehyde in PBS. Brains were post-fixed in the same solution, rinsed four times in a 0.2-M cacodylate/calcium chloride buffer, and again post-fixed for 4 h in 2% osmium tetroxide made in double-distilled water. After another four cacodylate/calcium chloride rinses, samples were stained with 1% uranyl acetate overnight. Samples were then washed three times in deionized H_2O and dehydrated with a graded series of ethanol solutions. Once fully dehydrated, samples were embedded in Epon. Ultrasectioning and transmission electron microscopy microscopy was performed by Nicholas H. Conoan (University of Nebraska, EM Core; see Acknowledgments).

Statistical analysis

Statistical analyses were performed using GraphPad Prism (ver. 7.02; GraphPad Software Inc., La Jolla, CA) and SPSS software (SPSS, Inc., Chicago, IL). A repeated-measures (RM) three-way analysis of variance (ANOVA) was conducted for the factors, CS, blast exposure, and time interval, as independent variables. For RM-ANOVA, a Greenhouse-Geisser correction was applied for the delayed fear conditioning, trace fear conditioning, and myelin density analyses. For MBP and CNPase optical density analyses, the CA1 area was divided into 10 layers representing the *stratum oriens*, *stratum pyramidale*, and *stratum radiatum* (Str. Ori 1, 2, 3, 4; Str. Pyr 1, 2; and Str. Rad 1, 2, 3, 4), and a two-way RM-ANOVA was performed for blast exposure and layer as variables. To facilitate readability, only statistically significant ($p < 0.05$) ANOVA results (main effect or interaction) are reported in the text.

Results

Advanced blast simulator exposures

The entire study used 471 shock-wave exposures, and, as described previously, the shockwave generated by the ABS mimicked a Friedlander curve.[51] See Figure 1 for an example. The mean peak incident overpressure was 15.32 ± 1.07 psi (mean ± standard deviation; ~105.6 kPa, coefficient of variation [COV] = 7%), with a positive (overpressure) phase of ~5.66 ms followed by an ~8.10-ms negative (underpressure) phase with peak pressure of −3.79 ± 0.26 psi (~26.1 kPa, COV = 7%). Impulse (the integration of pressure × time) was measured as 0.03490 ± 0.00478 psi·s (COV = 14%), and shock-wave velocity near the mouse was 473.30 ± 9.16 m/s (COV = 2%). Note that the second peak of ~24 psi, observed at time ≅ 1 μs after the initial peak (Fig. 1), was interpreted as a reflection wave from the animal holder toward the pencil gauge.

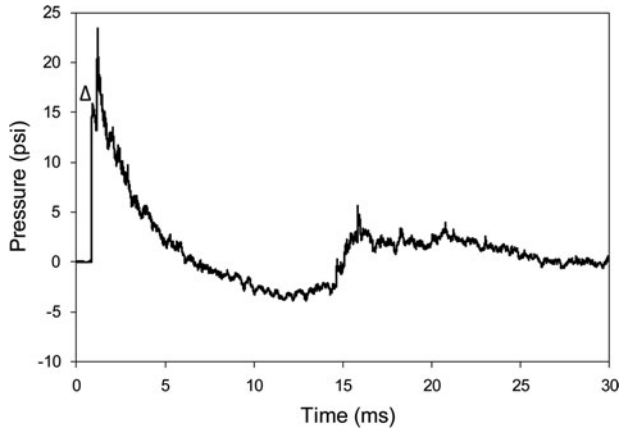

FIG. 1. Example of the time-pressure profile of a shockwave recorded near the head of the mouse. The shockwave (mean velocity 478.35 m/sec) was recorded by a pencil gauge positioned near the head of the animals. The initial ambient pressure (0 psi) increased to a mean peak positive pressure of 15.74 psi (seen adjacent to the small triangle, Δ), duration 5.31 ms, and impulse 0.04 psi•ms, followed by a peak negative pressure (–3.88 psi) phase of 8.48-ms duration. The maximum pressure attained of ~23 psi, seen as a secondary peak, results from a reflection of the incoming wave on the holder and adjacent instrumentation.

Mortality and body weight after blast

Figure 2 summarizes alterations in survival and body weight after treatment. All mice that received 1×or 4×Sham or 1×Blast survived. For 4×Blast mice, there was a gradual attrition as a function of number of blast exposures (Fig. 2A): 54.8% were alive by the final time point (chi-square survival analysis: $\chi^2 = 36.77$, $df = 1$, $^{***}p < 0.001$, $n = 72$ for 4×Sham and $n = 115$ for 4×Blast).

Figure 2B summarizes the body weight changes 24 h after 1×Sham or 1×Blast. The 1×Blast mice exhibited a 6.6% reduction in body weight and 1×Sham mice an ~0.5% reduction (Kruskal-Wallis analysis of variance, $H_{(1)} = 80.010$; $^{***}p < 0.001$). The 4×Sham mice exhibited a negligible decrease in weight over the 4-day blast procedure, whereas 4×Blast exhibited a 7.0–8.2% average loss in body weight (Fig. 2C; two-way ANOVA: blast×blast day interaction, $F_{(1.50,97.59)} = 19.11$; $^{***}p < 0.001$; blast $F_{(1,65)} = 107.704$; $^{***}p < 0.001$).

Prolonged self-righting reflex after anesthesia and blast

Figure 3 summarizes the length of time mice remained unconscious after sham or blast exposure. The 1×Sham mice exhibited a mean righting reflex duration of 51.4 sec, whereas 1×Blast mice had significantly longer periods of unconsciousness, averaging 338.7 sec (Kruskal-Wallis ANOVA for ranks, $H_{(1)} = 81.229$; $^{***}p < 0.001$; Fig. 3A). On each given day, 4×Blast mice had longer righting reflex durations (459.41, 379.17, 358.69, and 395.7 sec for day 1 to day 4, respectively) than 4×Sham mice (42.6, 44.13, 46.24, and 47.73 sec for day 1 to day 4, respectively; two-way RM-ANOVA: blast×blast day interaction, $F_{(2.54,350.10)} = 1.695$; blast, $F_{(1,138)} = 150.469$; $^{***}p < 0.001$; Fig. 3B).

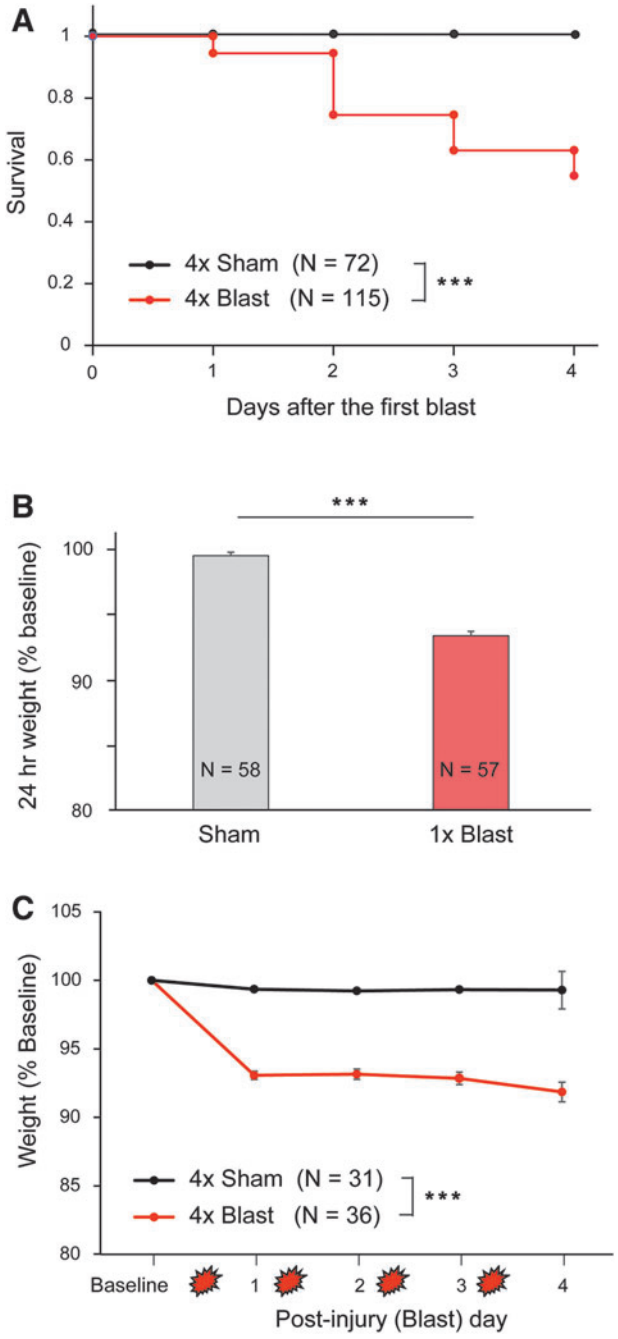

FIG. 2. Survival rates and body weight changes after blast. (**A**) Percentage of animals that survived after repeated exposures to blast. No animals expired from 1×or 4×Sham treatment or after 1×Blast. $n = 72$ for 4×Sham, $n = 115$ for 4×Blast. $n = 57$ for 1×Sham, and 1×Blast, data not shown. (**B**) Body weight change (percentage) after 1×Sham treatment ($n = 58$) or 1×blast ($n = 57$). Mice that sustained a single blast last weighed ~6.6% less than pre-blast baseline at 24 h after injury. $^{***}p < 0.001$. (**C**) Body weight changes at baseline and on days 1–4 after blast. The 4×Blast mice ($n = 36$) exhibited 7.0–8.2% losses of their body weight, whereas Sham mice ($n = 31$) remained stable (99.3% of baseline). The graph includes data for mice that survived all blast exposures. $^{***}p < 0.001$. Data are mean ± SEM. SEM, standard error of the mean. Color image is available online.

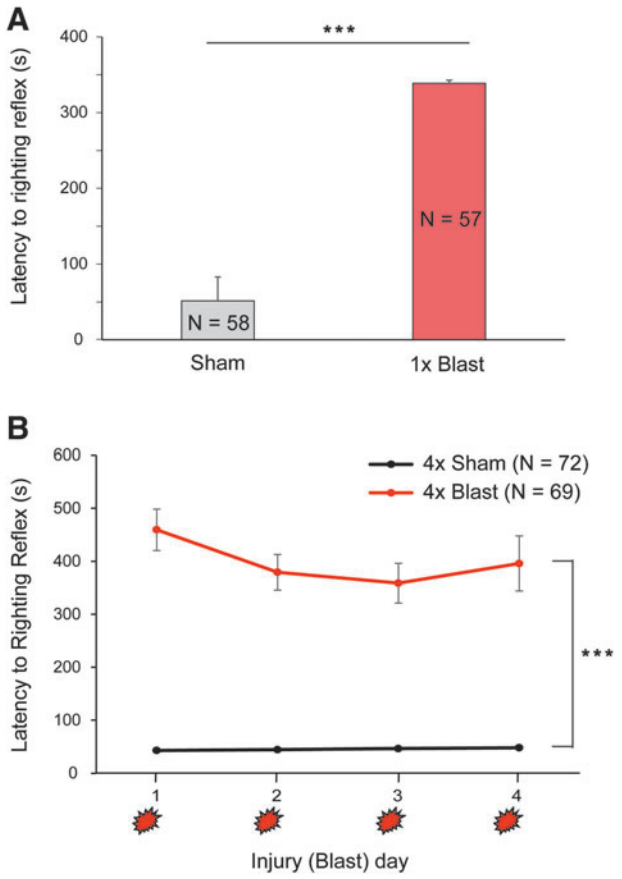

FIG. 3. Righting reflex after the blast. (**A**) Anesthetized mice exposed to 1×Blast ($n=57$) took longer to self-right than (also anesthetized) 1×Sham controls ($n=58$). ***$p<0.001$. (**B**) Mice exposed to 4×Blast ($n=69$) took longer to self-right than 4×Sham ($n=72$) on all 4 days of daily blast exposure. Main effect of blast, ***$p<0.001$. Data are mean ± SEM. SEM, standard error of the mean. Color image is available online.

Blast traumatic brain injury did not affect delay fear learning or extinction

To assess conditioned fear behavior after blast, separate groups of mice were tested in a cued (delay) fear conditioning paradigm at various time points up to 8 weeks after single or repeated blast exposure (Fig. 4A). A CS was temporally paired with footshock in Context A (conditioning), and then on day 2, mice were repeatedly (50×) presented with the CS without coincident footshock in Context B (extinction). On day 3, mice were tested for retrieval of the freezing to (5×) CS in Context B, and finally on a fear renewal test, in which animals were presented with the (3×) CS without footshock in Context A (Fig. 4A,B).

Single blast. Mice were tested for fear learning and extinction, as above, beginning 1, 2, 4, or 8 weeks after 1×Blast. Irrespective of post-blast interval, 1×Blast and 1×Sham mice showed a similar and significant increase in freezing across CS presentations during conditioning (three-way RM-ANOVA: interaction of CS×blast×post-blast interval, $F_{(3,45)}=0.0398$; $p=0.989$). At the 1-, 2-, 4-, and 8-week time points, respectively, the main effect of CS F ratio was all significantly different ($F_{(\text{d.f.=1, 12 or 1, 9 for 2 wk})}=$ 126.0, 220.4, 84.8, and 32.1; ***$p<0.001$). There was a significant decrease in freezing during extinction training (three-way RM-ANOVA: CS×blast×post-blast interval, $F_{(3,45)}=3.55$; *$p=0.0216$). For 1, 2, 4, and 8 weeks, respectively, the main effect of last five CS versus first five CS was $F_{(1,12)}=29.59$, 20.45, 22.00, and 16.84 (corresponding to ***$p<0.001$, **$p<0.01$, ***$p<0.001$, and **$p<0.01$), but there were no differences between 1×Sham and 1×Blast groups (Fig. 4B).

On the fear extinction retrieval test, there was a significant increase of freezing to the CS relative to baseline for all groups of animals, but, again, there were no group differences (three-way RM-ANOVA: CS×blast×post-blast interval, $F_{(3,45)}=0.238$; $p=0.869$). For 1, 2, 4, and 8 weeks, respectively, the main effect of CS (CS vs. baseline) was $F_{(1,12)}=97.97$, 37.16, 43.27, and 62.89 (all ***$p<0.001$). In the fear renewal test, the CS induced significantly more freezing over baseline, a difference that was similar for all groups (three-way RM-ANOVA: interaction of CS×blast×post-blast interval, $F_{(3,45)}=0.467$; $p=0.707$; main effect of CS vs. baseline, $F_{(1,12)}=62.89$, 74.41, 79.83, and 99.07; ***$p<0.001$; Fig. 4B). These data demonstrate that bTBI did not impair cued delay fear behavior or hearing, at least of a white noise, which replicates other studies in mice,[52] but is nonetheless noteworthy given clinical cases of impaired hearing after blast.[53]

Repeated blast. One explanation of the absence of 1×Blast effects on fear is that a single blast is insufficient to impair this behavior. To address this possibility, we performed the same fear paradigm 1, 2, or 8 weeks (each in a separate group of mice) after subjecting mice to *four* daily (one per day) blasts. At all of the post-blast intervals, the 4×Blast and 4×Sham groups showed a similar, significant increase in freezing during conditioning (three-way RM-ANOVA: CS×blast×post-blast interval, $F_{(2,89)}=1.29$; $p=$ 0.282; two-way ANOVA, main effect of CS: 1 week, $F_{(1,23)}=75.40$; ***$p<0.001$; 2 weeks, $F_{(1,27)}=145.1$; ***$p<0.001$; 8 weeks, $F_{(1,39)}=167.4$; ***$p<0.001$) and a similar, significant decrease during extinction training (three-way RM-ANOVA: CS×blast×post-blast interval, $F_{(2,89)}=0.308$; $p=0.736$: two-way RM-ANOVA, main effect of extinction [first five CSs vs. last five CSs]: 1 week, $F_{(1,23)}=38.28$; ***$p<0.001$; 2 weeks, $F_{(1,27)}=32.23$; ***$p<0.001$; 8 weeks, $F_{(1,39)}=62.73$; ***$p<0.001$), but, again, no difference between 4×Sham and 4×Blast groups (Fig. 4C).

On an extinction retrieval test, freezing of the 4×Blast group was again not different from 4×Shams at the 1- and 2-week post-blast intervals, but showed modest, significantly less freezing, relative to Shams, at 8 weeks after blast—suggesting either a

FIG. 4. Cued (delayed) fear conditioning/extinction was not affected by bTBI. (**A**) Schematic illustration of the cued fear conditioning/extinction task. Fear conditioning/extinction/retrieval/renewal tests (block of 3 days) were performed 1, 2, 4, and 8 weeks after 1×Blast and 3 days, 2 weeks, and 8 weeks after 4×Blast. The test sequence is described in the Methods. (**B**) Percent freezing data for 1, 2, 4, and 8 weeks after 1×Blast. $n=7$ for 1×Sham, and $n=7$ for 1×Blast at 1, 4, and 8 weeks. $n=6$ for 1×Sham and $n=5$ for 1×Blast at 2 weeks. COND, fear conditioning; EXT, extinction training; RET, retrieval test; REN; fear renewal test; BL, baseline; CS 03, third CS; CS 01–05, average of first five CSs; CS 45–50, average of last five CSs. (**C**) Percent freezing data for 3 days, 2 weeks, and 8 weeks after 4×Blast. $n=12$ for 4×Sham and $n=13$ for 4×Blast at 3 days, $n=15$ for 4×Sham and $n=22$ for 4×Blast at 2 weeks, $n=19$ for 4×Sham and $n=22$ for 4×Blast at 8 weeks. Data are mean ± SEM. bTBI, blast traumatic brain injury; CS, conditioned stimulus; SEM, standard error of the mean. Color image is available online.

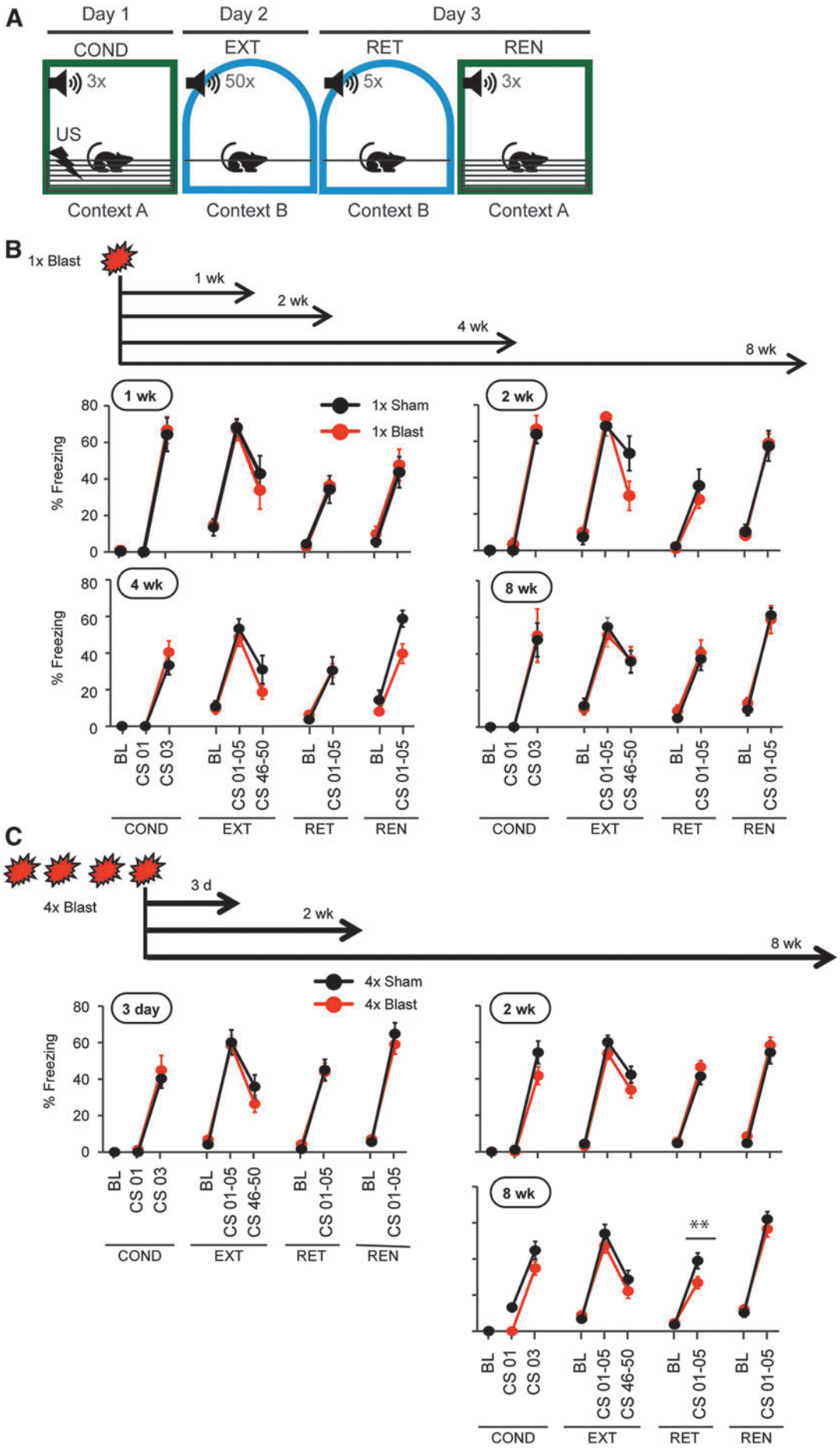
A
Day 1
Day 2
Day 3
COND
EXT
RET
REN
3x
50x
5x
3x
US
Context A
Context B
Context B
Context A
B
1x Blast
1 wk
2 wk
4 wk
8 wk
1 wk
2 wk
4 wk
8 wk
1x Sham
1x Blast
% Freezing
BL
CS 01
CS 03
CS 01-05
CS 46-50
COND
EXT
RET
REN
C
4x Blast
3 d
2 wk
8 wk
4x Sham
4x Blast
3 day
2 wk
8 wk
**

facilitation of extinction memory or a decay of the original fear memory (three-way RM-ANOVA: CS × blast × post-blast interval, $F_{(2,89)} = 2.73$; $p = 0.0707$; two-way RM-ANOVA for 8 weeks CS × blast interaction: $F_{(1,39)} = 8.23$; $^{**}p = 0.00663$; Fig. 4C). Finally, there were no group differences on the fear renewal test (Fig. 4C).

Overall, these data show that neither a single nor repeated exposure to blast produced deficits in the ability to acquire or extinguish a form of (delay) fear memory in which the CS and shock coterminate during conditioning.

Blast traumatic brain injury produced trace fear learning abnormalities

We next asked whether bTBI affected a variant of fear learning in which there is a 20-sec interval (''trace'') between the termination of the CS and the subsequent footshock during conditioning (Fig. 5A). The trace and delay variants of fear learning are known to recruit dissociable brain regions[54–56] and, as such, to be differentially affected by genetic mutations in molecules expressed in one of these regions, the hippocampus.[57] Mice were exposed to 1 × or 4 × Blast and tested for trace fear conditioning, retrieval, and context retrieval 1 or 8 weeks later. A separate cohort of 1 × or 4 × Blast mice were tested 3 days after blast to assess the behavior at a shorter post-injury interval (Fig. 5B).

Single blast. During conditioning and a subsequent retrieval test, freezing was measured during the pre-CS baseline, CS presentation periods, and the trace intervals between CS and (in the case of conditioning) footshock.

On the retrieval test on day 2, a three-way RM-ANOVA derived a significant three-factor interaction (three-way RM-ANOVA: interaction of blast × test phase [baseline, CS vs. trace] × post-blast interval, $F_{(3.72,67.03)} = 2.68$; $^{*}p = 0.042$). Separate analyses were performed for each test day. Freezing was significantly lower during the CS and trace, but not baseline, 3 days after 1 × Blast, relative to 1 × Sham controls (two-way RM-ANOVA: interaction of blast × test phase, $F_{(1.97,23.68)} = 10.99$; $^{***}p = 0.000439$; main effect of blast, $F_{(1,12)} = 14.30$; $^{**}p = 0.00262$; *post hoc* Fisher's least significant difference [LSD] tests for each period separately: baseline, $p = 0.441$; CS, $^{*}p = 0.0130$; trace, $^{***}p < 0.001$). One week after blast, freezing during the trace was slightly lower in the 1 × Blast group, and the interaction of the blast and test phase was significant (two-way RM-ANOVA: interaction of blast × test phase, $F_{(1.88,22.51)} = 3.76$; $^{*}p = 0.042$; main effect of blast, $F_{(1,12)} = 0.421$; $p = 0.529$). There were no group differences between the groups at baseline, CS, or trace at 8 weeks after blast (two-way RM-ANOVA: interaction for blast × test phase, $F_{(1.30,15.57)} = 0.0119$; $p = 0.953$; main effect of blast, $F_{(1,12)} = 0.126$; $p = 0.729$; Fig. 5C).

Repeated blast. Again, because the three-way RM-ANOVA for the blast × test phase × post-blast interval interaction was significant ($F_{(3.72,74.50)} = 2.78$; $^{*}p = 0.036$), separate two-factor ANOVAs were performed at the three post-blast intervals: 3 days, 1 week, and 8 weeks. As compared to the respective Sham controls, freezing during the trace was lower in the 3-day post-blast group (two-way RM-ANOVA interaction of blast × test phase, $F_{(1.73,\ 20.75)} = 9.26$; $^{**}p = 0.00193$; blast, $F_{(1,12)} = 0.126$; $p = 0.728$), not different at all periods in the 1-week group, and significantly lower during the CS periods in the 8-week group (two-way RM-ANOVA for blast × test phase: $F_{(1.64,16.39)} = 3.980$; $^{*}p = 0.0459$; *post hoc* Fisher's LSD tests for each test phase separately: baseline, $p = 0.585$; CS, $^{**}p = 0.0017$; trace, $p = 0.392$; Fig. 5C).

One interpretation of these results is that bTBI impairs the ability to bridge the CS and US when there is an interval between the two. Given that earlier work has shown that mice tend to freeze more at the start of the trace period (i.e., at CS offset) in anticipation of the footshock,[57–59] we calculated the difference between CS and trace freezing, [ΔFreezing (trace – CS)], during retrieval as an index of temporal bridging (Fig. 5D,E). This analysis revealed a greater trace and CS freezing differential, [ΔFreezing (trace – CS)], in 4 × Sham than 4 × Blast mice, which was strongest at 3 days, partially maintained at 1 week, and absent at 8 weeks after blast (repeated blast: two-way ANOVA interaction of blast × post-blast interval, $F_{(2,40)} = 4.40$; $^{**}p = 0.019$; main effect of blast, $F_{(2,40)} = 1.77$; $p = 0.313$; main effect of post-blast interval, $F_{(2,40)} = 0.964$; $p = 0.509$; *post hoc* *t*-test for 3 days, $^{***}p < 0.001$; 1 week, $p = 0.556$; 8 weeks, $p = 0.298$). These data indicate that after repeated blast exposures, this measure of temporal bridging was impaired at a time point relatively soon after blast (3 days), but recovered with time (by 8 weeks). For 1 × Blast, there was a similar time-dependent pattern, but this was not statistically significant (two-way ANOVA: interaction of blast × post-blast interval, $F_{(2,36)} = 2.62$; $p = 0.0868$; main effect of blast, $F_{(1,36)} = 4.43$; $p = 0.170$; main effect of interval, $F_{(2,36)} = 2.44$; $p = 0.291$).

These results for retrieval led us to apply the same, CS versus trace freezing differential, measure for conditioning. Here, all the Sham groups showed positive delta values, [ΔFreezing (trace – CS)], (greater freezing during trace than during CS) on the third and fourth pairings (Supplementary Fig. S1A,B), whereas all the Blast groups showed negative values, [ΔFreezing (trace – CS)], at the second pairing, with the 3-day post 4 × Blast group additionally showing a negative value at the third pairing. The difference, [ΔFreezing (trace – CS)], between corresponding Sham and Blast groups at the second and third parings was evident in the groups showing the greatest temporal bridging defects on the day 2 retrieval test (Fig. 5C). By the fourth trial, the 1 × and 4 × Blast groups showed positive values, [ΔFreezing (trace – CS)], similar to the level as corresponding Sham groups, suggesting that this temporal pattern learning dificit may arise from a one- or few-time learning experiences, and that the repetitive learning may compensate for this kind of deficit.

At 8 weeks after 4 × Blast, the 4 × Blast group froze less than the Sham animals during both the Trace and CS periods (two-way RM-ANOVA: test phase × blast interaction, $F_{(1.64,16.4)} = 3.98$; $^{*}p = 0.046$; Fig. 5C). At this post-blast time point, the 4 × Blast group also showed less freezing in the delay fear retrieval test compared to Sham controls (two–way RM-ANOVA: test phase × blast interaction, $F_{(1,39)} = 8.23$; $^{**}p = 0.00663$; Fig. 4C).

Last, there were no blast-group differences in freezing on a contextual fear test conducted the day after the trace retrieval test, irrespective of post-blast interval (Supplementary Fig. S1C), suggesting normal contextual fear and consistent with reports in a rat concussive injury model.[58]

Blast traumatic brain injury impaired spatial novelty preference but not social recognition

At the neural level, a key difference between delay and trace fear learning is that the latter form of conditioning is dependent on hippocampal function.[57] This led us to examine whether the impairments in trace fear produced by bTBI generalized to two other hippocampal-mediated behaviors: social recognition[46] and spatial novelty preference Y-maze[47] tests, that do not have a strong fear component.

Social recognition test. Mice investigated a novel juvenile male less during the test trial than during the preceding sample trial—indicative of social recognition (Fig. 6A). This pattern did

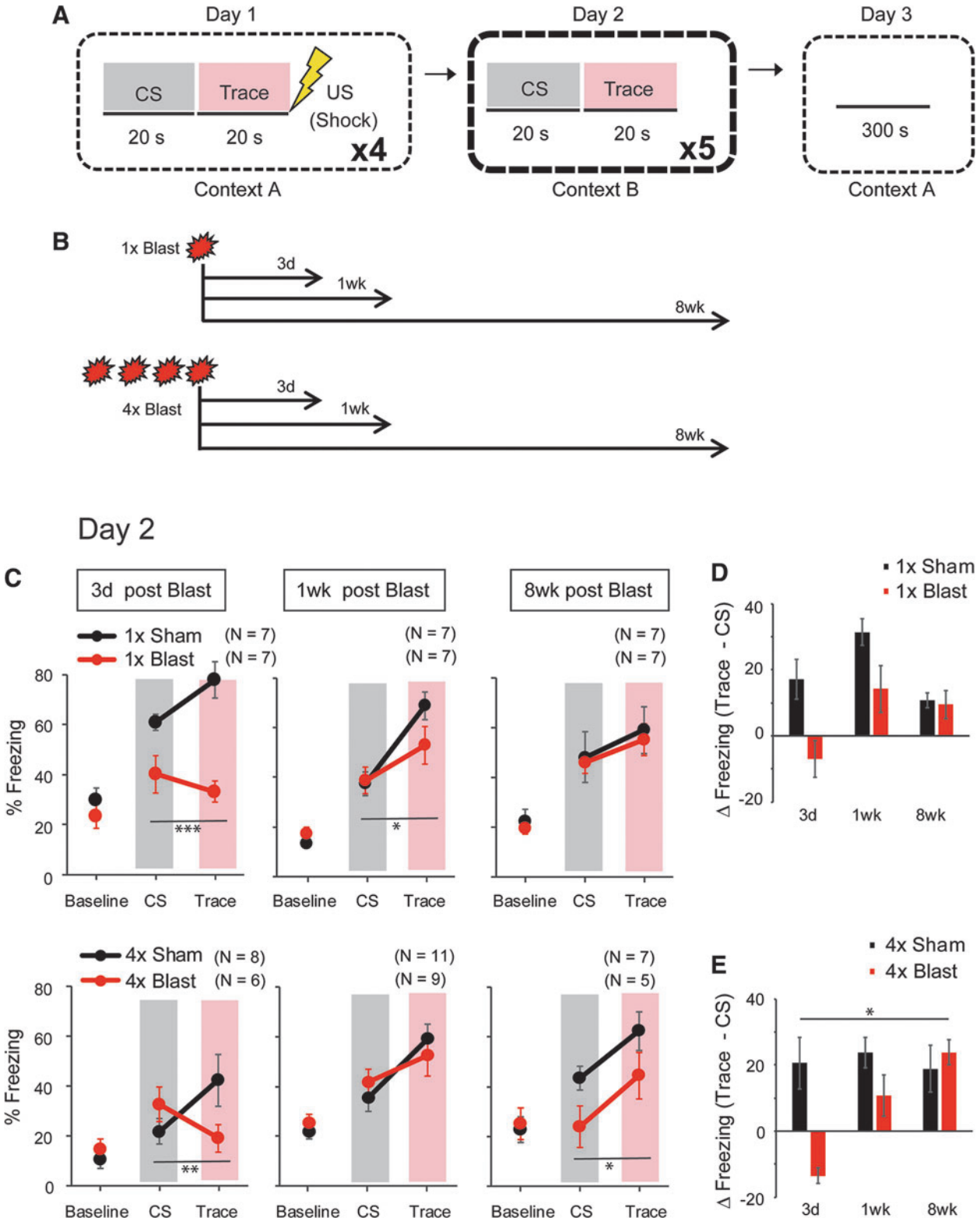

FIG. 5. bTBI produced abnormalities in trace fear learning. (**A**) Schematic illustration of the 3-day trace fear conditioning task. The trace period between CS and US was 20 sec. On day 1, there were 4×CS-trace-US sequences separated by a random interval (150–270 sec) between presentations. On day 2, there was no US; the 20-sec post-CS intervals are indicated as ''Trace'' periods. (**B**) Schematic illustration of the timeline of experiments after 1×Blast and 4×Blast. (**C**) Percent freezing during the trace fear retrieval test (day 2). Percent freezing during the pre-CS baseline, CS presentation, and trace period in mice conditioned either 3 days, 1 week, or 8 weeks after 1×Blast (top row) or 4×Blast (bottom row). $*p<0.05$; $**p<0.01$ for blast×test phase interaction. Gray shading indicates CS presentation, and pink shading indicates Trace period. (**D,E**) Trace and CS freezing differencial [ΔFreezing (trace – CS)], (% freezing during trace – % freezing during CS), are plotted to show the temporal pattern of freezing behavior after 1×Blast (D) and 4×Blast (E). $*p<0.05$ for blast×post-blast interval interaction. $n=7$ for 1×Sham and $n=7$ for 1×Blast at 3 days, 1 week, and 8 weeks, $n=8$ for 4×Sham and $n=6$ for 4×Blast at 3 days, $n=11$ for 4×Sham and $n=9$ for 4×Blast at 1 week, and $n=7$ for 4×Sham and $n=5$ for 4×Blast at 8 weeks. bTBI, blast traumatic brain injury; CS, conditioned stimulus; US, unconditioned stimulus. Color image is available online.

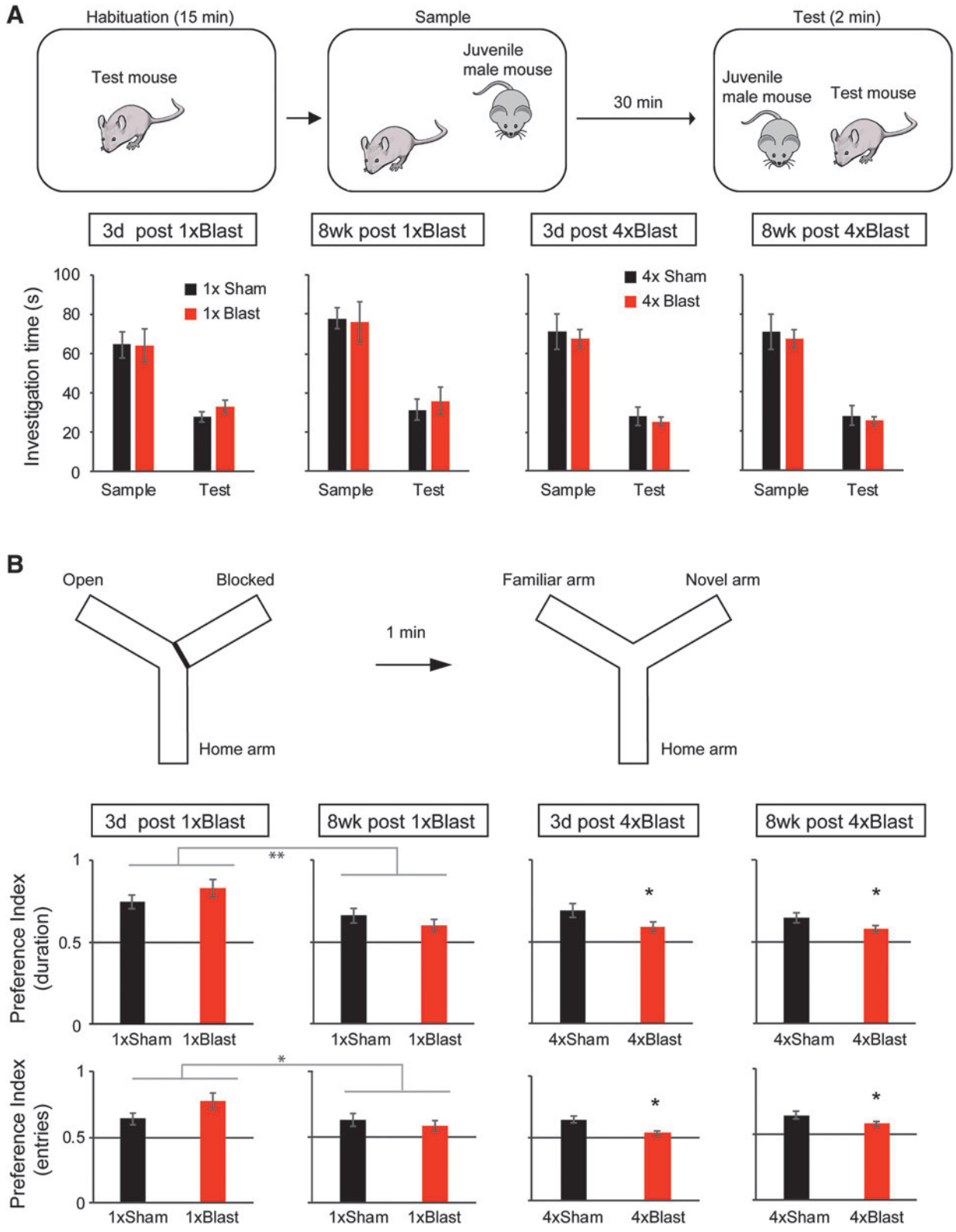

FIG. 6. bTBI impaired spatial novelty preference, but not social recognition. (**A**) Schematic illustration of the social recognition test (top) and accompanying results (bottom). Blast and Sham mice showed similar reductions in social investigation duration during the *test* trial, as compared to the *sample* trial. (**B**) Schematic illustration of spontaneous spatial novelty preference Y-maze test (top) and accompanying results (bottom). Preference indices for the novel arm, as measured by both *duration* (top graph row) and *#entries* (bottom graph row), showed a significant main effect of blast for 1×Blast and for 4×Blast. Preference index (duration) was above chance for Blast and Sham mice at all time points. Preference index (#entries) was above chance for Blast and Sham mice at time points except 8 weeks for 1×Blast and 3 days for 4×Blast mice. $^{**}p<0.01$; $^{*}p<0.05$. The number of mice for both the social recognition and Y-maze tests were: $n=7$ for 1×Sham and $n=7$ for 1×Blast for 3 days, $n=7$ for 1×Sham and $n=7$ for 1×Blast at 8 weeks, $n=11$ for 4×Sham and $n=9$ for 4×Blast at 3 days, and $n=7$ for 4×Sham and $n=5$ for 4×Blast at 8 weeks. Data are mean ± SEM. bTBI, blast traumatic brain injury; SEM, standard error of the mean. Color image is available online.

not differ between 1×or 4×Blast mice and their corresponding Sham groups, at 3 days or 8 weeks post-injury (three-way RM-ANOVA for 1×Blast: interaction of blast×test phase [sample trial vs. test trial]×post-blast interval, $F_{(1,23)}=0.0141$; $p=0.907$; main effect of test phase, $F_{(1,23)}=100.6$; $^{***}p<0.001$; for 4×Blast: interaction of blast×test phase×interval, $F_{(1,28)}=0.214$; $p=0.647$; main effect of test phase, $F_{(1,28)}=209.7$; $^{***}p<0.001$).

Y-maze spatial novelty preference test. The novel arm preference indices calculated from duration and number of arm entries during the first minute of the test trial (i.e., 1 min after the two-arm sample trial) were obtained as measures for spatial working memory. The 1×Blast mice did not show a difference in the preference index for duration nor number of entries in the novel arm, compared to 1×Sham controls (Fig. 6B). The preference index was lesser at 8 weeks than 3 days post-injury, as measured by novel arm relative duration (main effect of post-blast interval, $F_{(1,23)}=13.68$; $^{**}p=0.00118$) and the relative number of entries into the novel arm (main effect of post-blast interval, $F_{(1,23)}=4.33$; $^{*}p=0.049$), indicating an overall reduction in exploration of the novel arm for both the 1×Sham and 1×Blast groups at the 8-week time point compared to the 3-day time point.

For repeated blast, there was a significant difference between 4×Blast and 4×Sham controls for the preference index based on the novel arm exploration duration (two–way ANOVA of blast×post-blast interval: main effect of blast, $F_{(1,28)}=4.53$; $^{*}p=0.0423$). The 4×Blast mice also showed lower preference index based on the number of novel arm entries than 4×Sham control (main effect of blast, $F_{(1,28)}=4.60$; $^{*}p=0.0409$). All groups showed preference indices (preference to the novel arm) above chance (0.5; significant by one-sample *t*-test for all groups) when considering the duration in the novel versus familiar arm. Preference indices calculated based on arm *entries* were also above chance (significant by one-sample *t*-test) for all groups except the 1×Blast group at 8 weeks post-blast and the 4×Blast group at 3 days post-blast.

These data show that repeated, but not single, blast produced deficits in another measure of hippocampal-dependent cognition, spatial working memory.

Blast traumatic brain injury altered myelin and glia-related gene expression

We next examined the effects of bTBI on the expression of a suite of genes involved in myelin and glia function by performing RT-qPCR on tissue from the hippocampus (HPC), as well as other important nodes within the fear circuitry, including the medial prefrontal cortex (mPFC) and basolateral amygdala (BLA), and in two myelin-rich areas; the corpus callosum and anterior commissure. The expression of 11 genes was examined at 1, 2, 4, or 8 weeks after a single blast exposure and compared to corresponding levels in Sham controls.

This analysis revealed a number of gene-transcript-level alterations that varied as a function of brain region and post-blast (1×) interval (Fig. 7A). One of the clearest patterns was evident in the HPC for two genes associated with myelination, *Mbp* and *CNPase*, and two genes associated with axonal/nodes of Ranvier structure; neurofilament heavy chain (*Nefh*) and hyaluronan and proteoglycan link protein 2 (*Hapln2*; also known as *Bral1*).[60] All four genes were downregulated at 2–4 weeks, but not at 1 or 8 weeks, post-blast in the HPC (two-way ANOVA for the 2-week group: gene×blast interaction, $F_{(3.14,28.2)}=5.16$; $^{**}p=0.00519$; main effect of gene, $^{***}p=0.00274$; main effect of blast, $^{*}p=0.0215$; for the 4-week group: gene×blast, $F_{(3.11,37.3)}=3.26$; $^{*}p=0.0308$; main effect of blast, $^{*}p=0.0362$; Fig. 7B,C).

A different pattern was observed in the samples of the corpus callosum. At the later phase of assessment at 8 weeks after blast, all of the aforementioned myelin-related transcripts were elevated, as well as the proteoglycans, versican (*VCAN*), agrin, tenascin-R (*TNR*), neural/glial antigen 2 (*Ng2*), and G-protein-coupled receptor 17 (*GPR17*); a sensor of brain injury, and oligodendrocyte transcription factor 2 (*Olig2*); a transcription factor required for oligodendrocyte specification (two–way ANOVA for the 8-week group: gene×blast interaction, $F_{(3.76,45.1)}=0.917$; $p=0.458$; main effect of gene, $p=0.071$; main effect of blast, $^{**}p=0.00725$; Fig. 7B,D).

These data indicate dynamic alterations in the expression of 1) myelin and nodes of Ranvier-related genes in the HPC in the period 2–4 weeks after blast and 2) glial-differentiation and extracellular matrix (ECM)-related genes in corpus collosum 8 weeks after blast.

Blast traumatic brain injury reduced myelin marker proteins in the hippocampus

Based on the finding that bTBI altered myelin-related gene expression, we next performed immunostaining to determine whether there were injury-induced changes at the protein level for the myelin-associated molecules, MBP and CNPase (Fig. 8A,B,E). We focused on the hippocampus based on the prominent gene expression changes observed in this region (Fig. 7C), together with trace fear deficits (Fig. 5) and Y-maze deficits (Fig. 6B) resulting from bTBI.

Results showed that immunofluorescence signal intensity for MBP was significantly lower in the single-bTBI group (Fig. 8A,B), relative to Sham controls, in the CA1 region of the hippocampus 1 week (two-way RM-ANOVA: blast×layer interaction, $F_{(1.91,26.74)}=1.265$; $p=0.297$; main effect of blast, $F_{(1,14)}=5.952$; $^{*}p=0.029$), but not at 2 weeks, after blast (two-way RM-ANOVA: interaction,

FIG. 7. bTBI altered hippocampal expression of myelin and nodes of Ranvier-related genes. (**A**) Timeline of brain tissue dissections after 1×Blast. (**B**) RT-qPCR data for anterior commissure (AC), corpus callosum (CC), basolateral amygdala (BLA), pre-frontal cortex (PFC), and hippocampus (HPC). Illustrations of the sampled brain areas are shown as circles within the brain region cartoons at the top of each table. ΔC_T values from qPCR (the difference in Ct between target genes and reference genes) were calculated, and the normalized $2^{-\Delta\Delta Ct}$ values ($\Delta\Delta C_T$ is a difference in C_T between 1×Blast mice [$n=7$] the 1×Sham group [$n=7$]) are shown in a heatmap (cold for values <1.0; warm for values >1.0). (**C**) Summary of gene expression changes after a single blast for *MBP*, *CNPase*, *Nefh*, and *Hapln2* in the hippocampus; thick line indicates the average±SEM. (**D**) Summary of expression changes for 12 genes in the corpus callosum after 1×Blast; thick line indicates the average±SEM. bTBI, blast traumatic brain injury; *CNPase*, 2′,3-cyclic nucleotide-3-phosphodiesterase; Ct, cycle threshold; *Hapln2*, hyaluronan and proteoglycan link protein 2; *MBP*, myelin basic protein; *Nefh*, neurofilament heavy chain; qPCR, quantitative polymerase chain reaction; RT-qPCR, reverse-transcription quantitative real-time polymerase chain reaction; SEM, standard error of the mean. Color image is available online.

B

AC

	1wk	2wk	4wk	8wk
GFAP	1.11	2.14	1.32	1.05
AQP4	1.14	0.83	1.21	1.06
MBP	1.01	1.20	1.48	0.88
CNPase	0.99	1.15	1.18	0.81
Nefh	0.99	1.16	1.23	1.38
Hapln2	1.20	1.21	1.54	0.99
Vcan	1.08	1.05	0.94	0.87
Agrin	0.95	1.24	1.02	1.00
TN-R	1.04	1.12	1.06	1.17
Olig2		0.86	1.40	0.96
Gpr17	0.92	1.27	1.50	0.84
NG2	1.01	1.37	1.43	1.19

CC

	1wk	2wk	4wk	8wk
GFAP	1.31	0.83	1.18	1.76
AQP4	1.01	0.56	1.02	1.59
MBP	1.14	0.98	1.08	1.62
CNPase	0.87	0.79	1.02	1.57
Nefh	0.98	0.79	0.88	1.18
Hapln2	1.29	0.92	1.24	1.53
Vcan	0.98	1.24	1.44	1.28
Agrin	0.96	0.98	1.25	1.80
TNR	1.06	0.92	0.91	1.28
Olig2	0.88	0.88	1.16	1.54
Gpr17	0.95	0.93	1.12	1.23
NG2	1.03	0.66	1.02	1.38

BLA

	1wk	2wk	4wk	8wk
GFAP	1.40	0.90	1.35	0.83
AQP4	1.33	1.05	1.11	0.82
MBP	1.43	0.98	1.29	0.55
CNPase	0.71	1.45	1.26	0.99
Nefh	1.02	0.54	1.58	0.81
Hapln2	1.93	1.00	1.35	0.63
Vcan	0.89	1.34	0.98	1.01
Agrin	1.58	1.30	1.16	1.13
TNR	1.41	1.30	1.24	1.10
Olig2	0.81	1.06	1.26	0.90
Gpr17	1.06	1.04	1.22	1.02
NG2	1.09	1.07	1.09	1.18

2.0 1.0 0.3

PFC

	1wk	2wk	4wk	8wk
GFAP	1.01	0.85	1.02	1.37
AQP4	0.98	1.10	0.97	1.15
MBP	0.70	0.71	0.63	2.01
CNPase	0.94	0.71	0.68	0.96
Nefh	0.94	1.14	0.88	0.84
Hapln2	0.75	0.72	0.52	1.67
Vcan	0.90	0.67	0.88	1.24
Agrin	0.98	1.25	0.78	1.26
TNR	1.25	1.26	0.80	0.96
Olig2	0.84	1.06	0.85	1.49
Gpr17	0.96	0.90	0.98	1.19
NG2	1.02	1.19	0.94	1.09

HPC

	1wk	2wk	4wk	8wk
GFAP	1.04	0.88	1.10	1.15
AQP4	1.42	0.90	1.10	1.17
MBP	1.37	1.53	0.68	0.93
CNPase	1.06	1.38	0.67	0.82
Nefh	1.36	1.73	0.72	0.93
Hapln2	1.34	1.69	0.68	0.86
Vcan	1.03	1.08	1.05	1.26
Agrin	1.11	1.06	0.82	0.98
TNR	0.94	0.87	1.31	1.25
Olig2	1.14	1.40	0.76	0.99
Gpr17	1.04	0.92	0.81	0.97
NG2	1.16	1.13	0.95	1.20

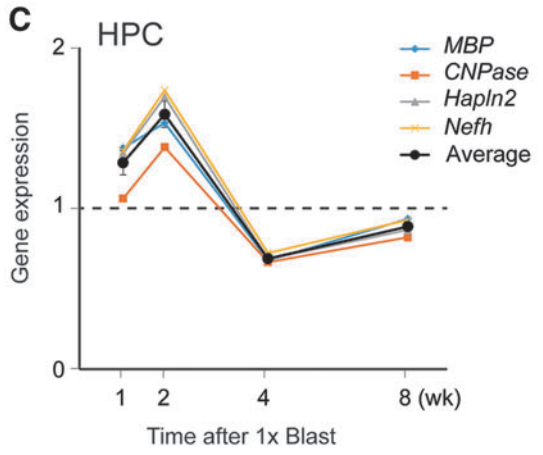

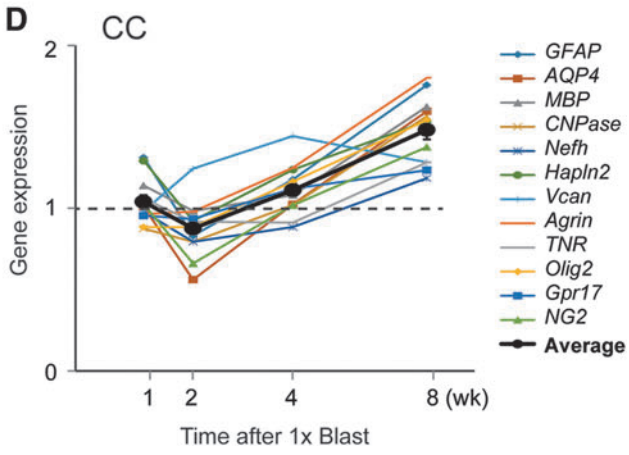

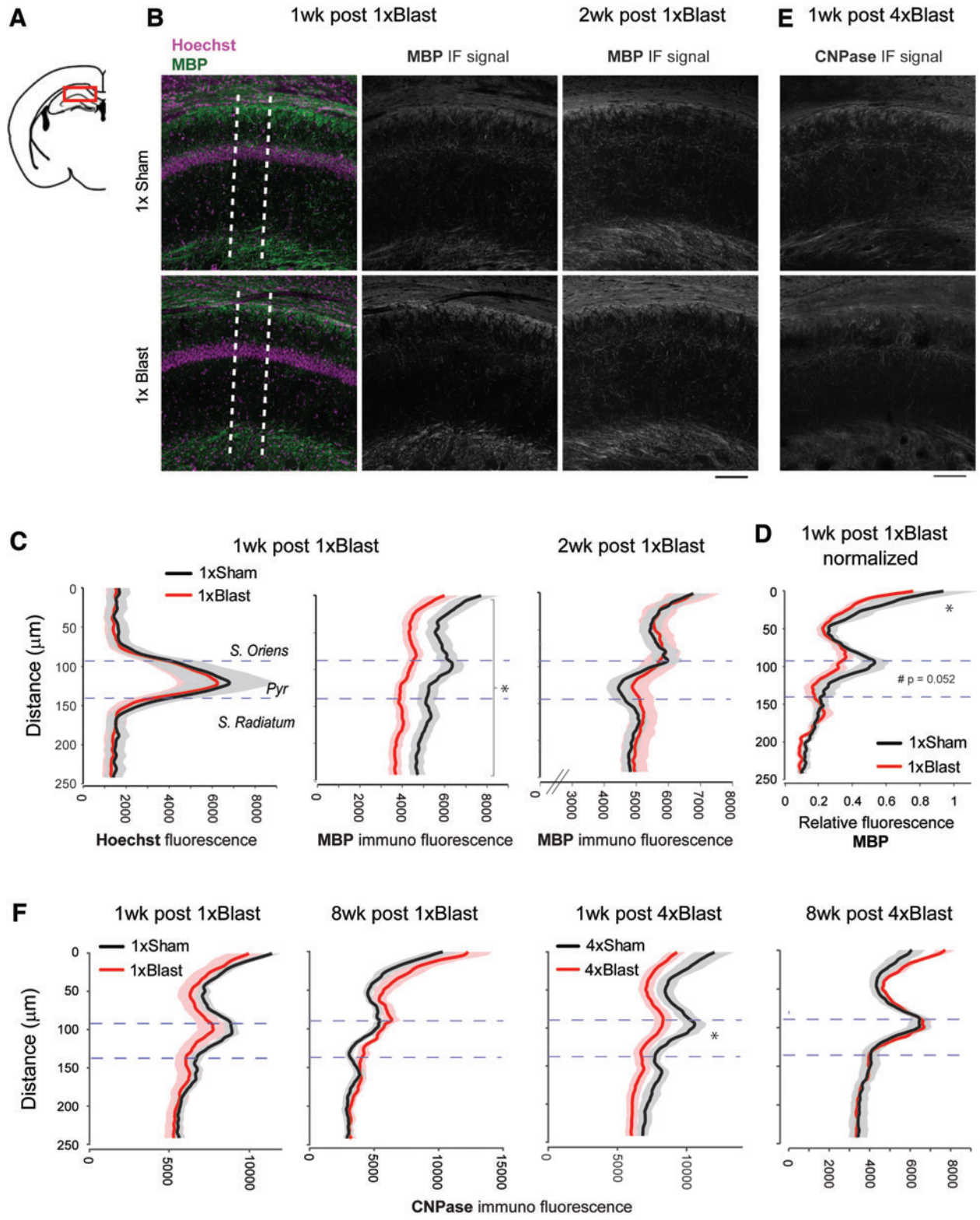

FIG. 8. bTBI reduced hippocampal protein levels of myelin markers. (**A**) Illustration of a coronal section (bregma −1.94 mm) containing the HPC CA1 area examined. (**B**) Representative images of MBP immunostaining images at 1 and 2 weeks after 1 × Blast. Dotted lines indicate an example of the zone (200 μm thick) within which the immunofluorescent signal was analyzed. (**C**) Quantification of MBP signal intensity at 1 and 2 weeks after 1 × Blast. The intensity curve for Hoechst nuclear staining (left) was used to define the pyramidal cell layer. Dotted horizontal lines represent the pyramidal cell layer. $n = 8$ for 1 × Sham and $n = 8$ for 1 × Blast at 1 and 2 weeks. $^{*}p < 0.05$, main effect of blast. (**D**) Normalized relative fluorescence of MBP signal for 1 week post 1 × Blast. $^{*}p < 0.05$; $^{\#}$subthreshold significance. (**E**) Representative images of CNPase immunostaining images at 1 week after 4 × Blast. (**F**) Quantification of CNPase immunofluorescence signal intensity at 1 and 8 weeks after 1 × Blast and 4 × Blast. $n = 7$ for 1 × Sham and $n = 7$ for 4 × Blast at 1 and 8 weeks. $^{*}p < 0.05$, blast × layer interaction. Data are mean ± SEM (shade). Scale bar, 100 μm. bTBI, blast traumatic brain injury; CNPase, 2′,3-cyclic nucleotide-3-phosphodiesterase; IF, immunoflourescence; MBP, myelin basic protein; SEM, standard error of the mean. Color image is available online.

$F_{(1.76,22.91)} = 1.09$; $p = 0.346$; blast, $F_{(1,13)} = 0.0152$; $p = 0.904$; Fig. 8C). Closer inspection of the patterns of fluorescence indicated that, within the CA1 region, the greatest reductions were in the dorsal *stratum oriens* (two-way RM-ANOVA: blast × layer interaction, $F_{(2.71,37.96)} = 1.36$; $p = 0.270$; Fisher's LSD test: *stratum oriens* [top layer], $^*p = 0.027$; *stratum pyramidale* [top layer], $p = 0.0522$; Fig. 8D). To substantiate these findings, we stained alternate sections from the same mice with the myelin staining dye, Black Gold II, and found the same patterns of myelin loss at 1 week ($^*p < 0.05$, *t*-test), not at 2 weeks, after bTBI (Fig. 9).

To extend these data, we quantified hippocampal levels of another myelin marker, CNPase, which is present in non-compact

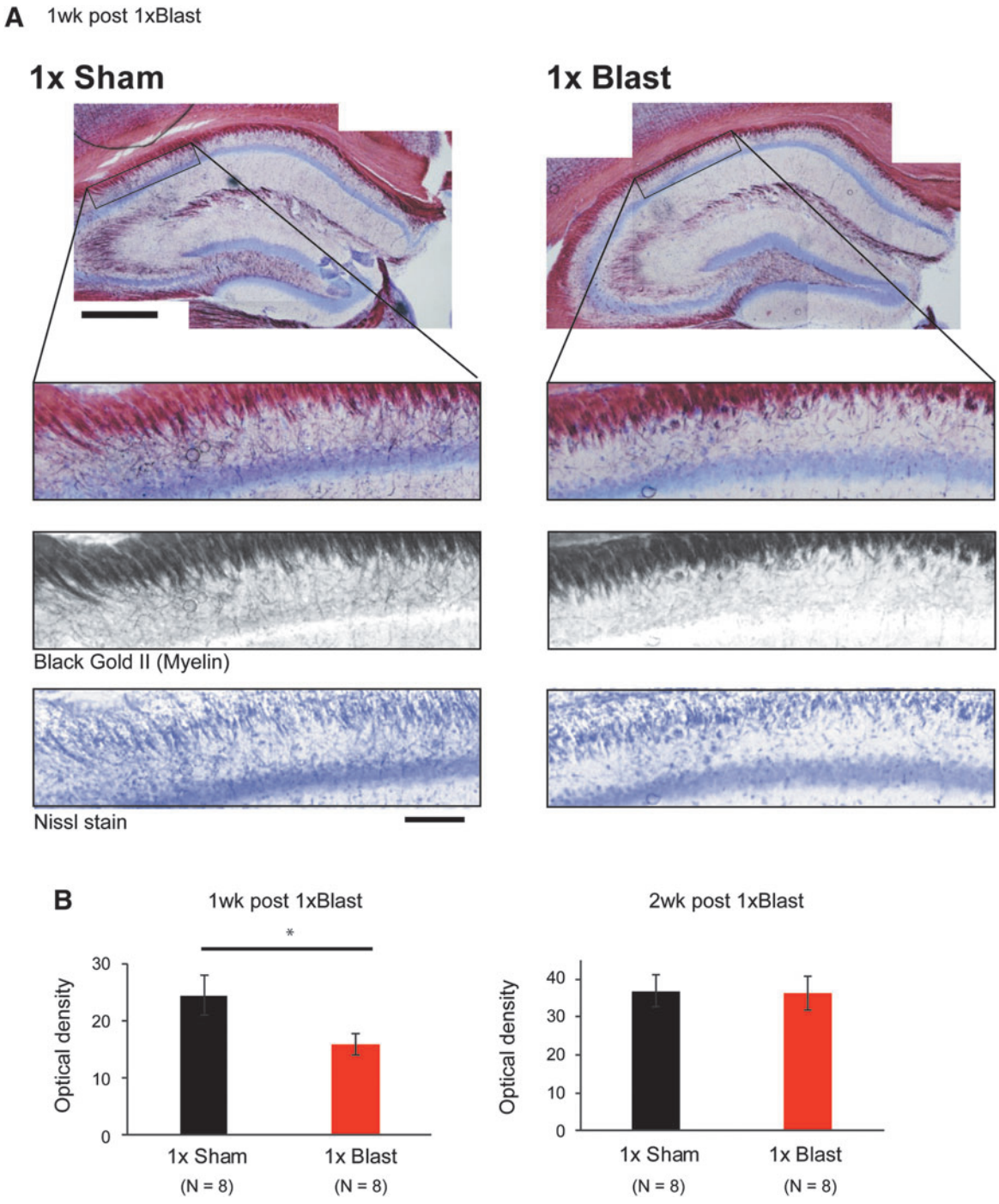

FIG. 9. bTBI produced loss of hippocampal myelin. (**A**) Top: representative image of histological myelin staining using Black Gold II, costained with cresyl violet (Nissl staining), for 1 × Sham and 1 × Blast at 1 week. Scale bar, 500 μm. Black rectangles indicate areas where myelin signals were analyzed. Bottom: magnified view of *striatum oriens*. From top to bottom: brightfield, Black Gold II, and Nissl stain images, respectively. Scale bar, 100 μm. (**B**) Quantification of Black Gold II staining intensity in the CA1 striatum oriens revealed reduced myelin in 1 × Blast ($n = 8$), as compared to 1 × Sham ($n = 8$) mice at 1 week, but not at 2 weeks, post-blast ($n = 8$ for 1 × Sham, $n = 8$ for 1 × Blast). $^*p < 0.05$. Data are mean ± SEM. bTBI, blast traumatic brain injury; CA1, *cornu ammonis* 1; SEM, standard error of the mean. Color image is available online.

myelin sheets[61] and can reflect perturbations in oligodendrocyte maturation, whereas MBP, for example, is present only in mature oligodendrocytes and compact myelin.[62,63] We examined CNPase at 1 week after 1×blast, as well as 8 weeks post-blast, to determine whether the recovery in myelin was long-lasting. There was a non-significant trend in reduction of CNPase at the 1-week, but not 8-week, interval (Fig., 8F). Next, we examined CNPase expression at the same intervals after repeated blast and found that expression was significantly decreased relative to Sham controls at 1 week (two-way RM-ANOVA: blast×cell layer interaction, $F_{(1,15)}=5.34$; $*p=0.028$; main effect of blast, $F_{(1,15)}=3.37$; $p=0.086$), but not at 8 weeks (interaction, $F_{(1,10)}=0.481$; $p=0.504$; blast, $F_{(1,10)}=0.106$; $p=0.752$), after blast (Fig. 8F). Finally, GFAP immunostaining was performed and the areal density of GFAP-positive astrocytes quantified; there was no difference between single-Blast mice and Sham controls for GFAP-positive cell density in hippocampal CA1 nor in the hilar region of the dentate gyrus (Supplementary Fig. S2).

Together, these data complement and extend the results of our gene expression analysis by showing that bTBI produces decrements in hippocampal levels of key myelin-related proteins, MBP and CNPase.

Blast traumatic brain injury causes damage to myelin in the corpus callosum

Our gene expression analysis revealed blast-related changes for *Hapln2 and Nefh*, two genes associated with the structure of the nodes of Ranvier.[60] Therefore, we examined the nodes of Ranvier through a combination of immunostaining for the paranodal marker, contactin-associated protein (Caspr), and a nodal gap marker, Nav1.6.[64] For these analyses, we first examined the central part (close to midline) of the corpus callosum because of the difficulty in examining nodes in neuronal-rich regions such as the hippocampus. Nodes were inspected for gap length, paranodal length, number of bundles, and curvature. An initial examination of images obtained with a fluorescence microscope showed that mice exposed to repeated blast had significantly longer nodal gap length 1 and 8 weeks after 4×Blast, as compared to Sham controls (Kolmogorov-Smirnov test on pooled data from Sham and Blast groups: 1 week after 4×Blast, $*p=0.0175$; 8 weeks after 4×Blast, $*p=0.0213$; Fig. 10B–D).

There was also an alteration in mRNA levels of glial, ECM, and myelin-related genes in the corpus callosum after blast, which was significant at 8 weeks after 1×Blast (Fig. 7D). At this time point, all 12 of the sampled transcripts were elevated in Blast mice compared to Sham controls, with 11 of the 12 transcripts exhibiting increases >20%. These data are consistent with previous evidence that TBI can disrupt the structural connectivity of the corpus callosum.[65]

To provide preliminary support for these data at the electron microscope level, we obtained high-resolution images of the corpus callosum from one representative 4×Blast–exposed mouse (and corresponding Sham control) at the 1- and 8-week post-blast intervals. These ultrastructural images revealed the presence of vacuoles and evidence of axonal damage 1 week after 4×Blast. These changes included increased paranodal gap distance and indications of redundant myelin (i.e., excessively long myelin that did not tightly wrap axons and occasionally folded back onto itself),[66,67] loosely packed myelin around axons, axons with protrusions, and abnormally thickened myelin (Fig. 10E and Supplementary Fig. S3A). With the exception of increased paranodal gap distance, the rest of these changes were not apparent at 8 weeks after 4×Blast (Fig. 10E). Finally, examination of hippocampal tissue indicated more vacuoles around axons of 4×Blast mice, relative to Sham controls, at both the 1- and 8-week post-blast time points (Supplementary Fig. S3B).

Discussion

The results of the current study showed that blast injury in mice produced an array of behavioral, molecular, and structural changes that varied as a function of the number of blast episodes and the time post-injury (Fig. 11). The study adopted a method of TBI produced by blast-wave exposure previously shown to produce transient decreases in home-cage activity when C57BL/6J mice are exposed to a single blast.[15] We extended this method by applying a regimen of daily blast over 4 consecutive days. It should be noted that though we sought to examine the effects of repeated blast exposure in a manner (daily) that was systematic, consistent, and replicable in future studies, this is an experimental preparation that, by necessity, relates more closely to some, but not other, real-world, including military, scenarios—given that the experience of repeated blast in such settings is typically sporadic and random. Nonetheless, it will be interesting to examine the consequences of varying the number and spacing of repeated blast in future work to model various injury scenarios. This follow-up research could also shed light on the precise cause of the fatalities after the repeated blast, which probably reflects damage to the vascular system, lungs, and other soft tissues.

At the behavioral level, we did not find alterations in ''delay'' (US coterminates with the CS) form of fear conditioning (or extinction) after either single or repeated blast. This finding agrees with the absence of effects on these behavioral measures in C57BL/6 mice and rats that have suffered blast-induced mTBI[52] or concussion-induced TBI.[58,68,69] Whereas one study reported an impairment in delay cued fear extinction in C57BL/6 mice after single blast,[70] this required high (50–60 psi) blast pressure. Other studies in rats found a deficit when blast exposure occurred between

FIG. 10. bTBI altered the structure of the nodes of Ranvier in the corpus callosum. (**A**) Illustration of a coronal section (bregma +0.5 mm) containing the corpus callosum region examined. (**B**) Representative images of nodes of Ranvier staining with anti-Caspr and anti-Nav1.6 antibodies at 8 weeks after 4×Blast. Scale bar, 5 μm. (**C**) Quantification of nodal gap length for 1×Blast ($n=7$) and 4×Blast ($n=7$) at 1 and 8 weeks. $n=9$ for 4×Sham and $n=8$ for 4×Blast at 1 week, $n=7$ for 4×Sham and $n=6$ for 4×Blast at 8 weeks. (**D**) Cumulative percentage analysis of nodal gap length for 4×Blast at 1 and 8 weeks. $*p<0.05$, Kolmogorov-Smirnov test. $n=83$, 107, 71, and 87 for 1 week after 4×Sham, 4×Blast, 8 weeks after 4×Sham, 4×Blast, respectively. (**E**) Electron micrographs of nodes of Ranvier in the corpus callosum for 1 week (top) and 8 weeks (bottom) after 4×Sham and 4×Blast mice. Filled arrowheads indicate the nodal gap and paranodal borders. Open arrowheads show distorted paranodal morphology in 4×Blast mice. Scale bars, 100 nm for 1 week after 4×Sham (example 2) and 8 weeks after 4×Blast (example 2); 500 nm for all other images (embedded in original micrographs). bTBI, blast traumatic brain injury; Caspr, contactin-associated protein. Color image is available online.

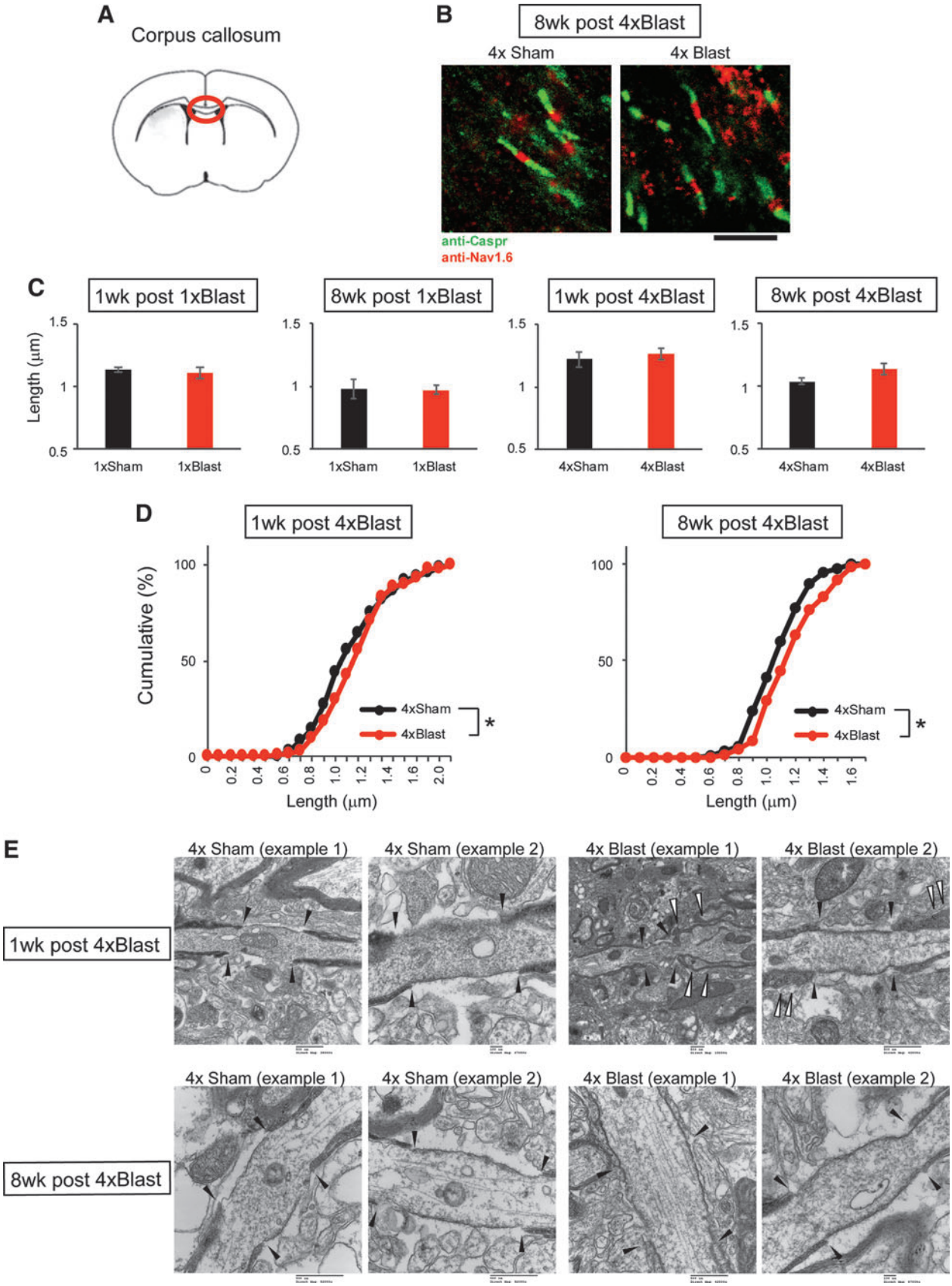
A
Corpus callosum
B
8wk post 4xBlast
4x Sham
4x Blast
anti-Caspr
anti-Nav1.6
C
1wk post 1xBlast
8wk post 1xBlast
1wk post 4xBlast
8wk post 4xBlast
Length (μm)
1xSham
1xBlast
4xSham
4xBlast
D
1wk post 4xBlast
8wk post 4xBlast
Cumulative (%)
Length (μm)
4xSham
4xBlast
*
E
1wk post 4xBlast
8wk post 4xBlast
4x Sham (example 1)
4x Sham (example 2)
4x Blast (example 1)
4x Blast (example 2)

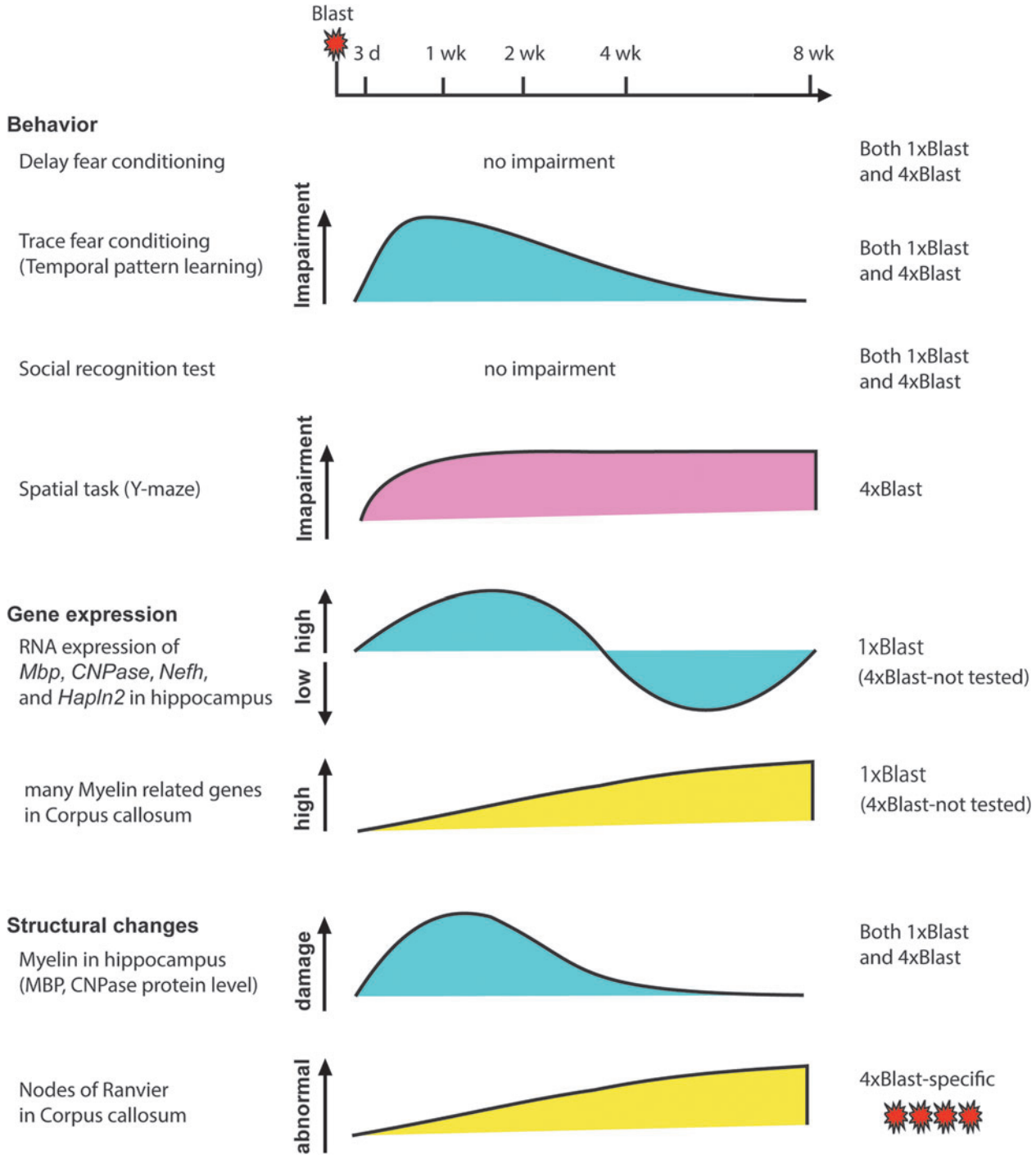

FIG. 11. Graphical summary of the main findings. Summary of time-dependent behavior, gene expression analysis, and structural analysis (protein and morphological) after blast. Trace fear abnormalities paralleled the time course of myelin structural changes after single and repeated blast, whereas spatial novelty preference deficits and structural change in the nodes of Ranvier and corpus callosum axons were evident only after repeated blast. *CNPase*, 2′,3-cyclic nucleotide-3-phosphodiesterase; *Hapln2*, hyaluronan and proteoglycan link protein 2; *Mbp*, myelin basic protein; *Nefh*, neurofilament heavy polypeptide. Color image is available online.

conditioning and testing,[24] or when conditioning took place at a prolonged interval after blast (>4 months).[25,71–73] Thus, together with the current findings, it appears that across rats and mice, mild (15 psi) bTBI has minimal effects on delay fear in the first 2 months after injury.

Several studies have now shown that blast produces significant changes in BLA neuronal density and dendritic morphology and alters the expression of various genes and molecules in the BLA.[25,74–76] Delay fear conditioning and extinction is heavily reliant on the BLA.[77,78] However, the lack of bTBI effects on delay fear conditioning suggests that if blast produced changes in BLA function, these were not sufficient to cause demonstrable impairment in this form of learning. Unlike delay fear, trace fear conditioning (in which the US occurs at the interval after CS

termination) is dependent on intact hippocampal function.[57] Interestingly, in this context, and echoing a recent study which found that single blast affected trace fear conditioning to a greater extent than delay conditioning in C57BL/6 mice,[52] we did find that mice exposed to single or repeated blast exhibited performance abnormalities in trace fear. Specifically, whereas cue-related freezing *per se* was not decreased after blast, mice subjected to single and repeated blast showed a lesser differential in freezing [ΔFreezing (trace – CS)] than sham during retrieval and conditioning.

This pattern, which was evident at relatively recent time points after blast (3 days and 1, but not 8, weeks), suggests a deficit in the ability to temporally bridge the interval from CS to the expected US, that is, an impairment in ''temporal pattern learning.'' The possibility that this behavioral abnormality reflects a deficit in hippocampal function is supported by the finding that repeated blast also impaired performance on the Y-maze spatial working memory task, another hippocampal-dependent task.[47] However, we found that a third hippocampal-dependent task, social recognition, was unaltered by blast. Hence, based on the current results and earlier works,[79] it appears that the effects of blast on hippocampal-dependent cognitive performance varies across tasks, likely attributable to differences in the sensitivity of different assays to the deleterious impact of blast.

There is a growing consensus that one of the main neural insults produced by TBI is axonal injury and disturbances in white matter.[52,70,80] In an attempt to provide a further link between the behavioral and neural effects of blast injury, we found that a single blast produced myelin damage in the hippocampus, whereas repeated blast exposure caused an increase in nodal gap length measured 1 or 8 weeks after blast. Nodal gap length, paranodal length, and nodal thickness are tightly regulated and undergo constant molecular remodeling,[81–83] including repair processes, after axonal insult.[84] Concussive TBI has been shown to cause damage to the nodes of Ranvier,[85] and morphological abnormalities of the nodes are also associated with a variety of behavioral abnormalities, including depression, autism, and cognitive impairment.[86–88] Indeed, there is growing evidence that myelin is critical for supporting cognitive functions, including contextual fear.[89–91]

Extending these data further, we found gene expression alterations in myelin and axon-related mRNA transcripts in the hippocampus and corpus callosum. Specifically, *Mbp* and *CNPase*, which are present in myelin and oligodendrocytes, and two genes, *Hapln2 and Nefh*, associated with the structure of the nodes of Ranvier[60] showed upregulation 2 weeks after a single blast exposure (repeated blast was not tested) and then downregulation at the 4- and 8-week post-blast time points. In parallel with these gene expression changes, MBP and CNPase protein levels were reduced in the *stratum oriens* of the hippocampus CA1 area 1 week after single or repeated blast. However, unlike the persistent gene expression changes, these protein levels had normalized by later post-blast time points. This could potentially reflect remyelination given that there was some indication of hippocampal oligodendrocyte precursor proliferation in the form of *Olig2* and *Ng2* gene expression increases within the first week after blast. Further analyses will be required to test this hypothesis, including examination of the protein levels of Olig2 and Ng2, as well as markers for mature oligodendrocytes such as Cc-1.

Additional studies will also be needed to determine the mechanism through which blast could produce such damage. One possibility is that blast causes axonal injury through the intense energy and overpressure passing through brain lipid-rich structures vulnerable to heat and mechanical damage. These mechanical effects could be amplified with repeated blast if the brain is rendered increasingly sensitive and vulnerable to multiple shockwaves.[92,93] In support of this notion, diffusion tensor imaging in rats has shown that repetitive blast exposure caused greater white matter tissue damage[94] than a single blast.[95] However, although the current study provides further preliminary support for a link between bTBI, myelin damage, and impaired cognition, a causal connection remains to be demonstrated by, for example, testing whether recovery of myelin[96–100] can reverse bTBI-induced trace fear abnormalities.

In conclusion, the current study examined the effects of single and repeated blast exposure in mice on various behavioral assays, as well as multiple genetic, molecular, and structural indices in the brain. The main findings were that blast-induced mTBI produced a specific set of behavioral disturbances, characterized by abnormal temporal organization of cue-induced freezing behavior in a conditioned trace fear test and deficient spatial working memory performance in a Y-maze task. bTBI was associated with changes in myelin-related gene expression and myelin and axonal damage in the hippocampus and corpus callosum. The behavioral and neural sequalae of bTBI occurred in a manner that varied depending on both the number of blast exposures and the time interval after blast. Together, our findings provide preliminary evidence supporting a link between bTBI-induced neural and cognitive impairment that may be of relevance to understanding the clinical course and potential opportunities for recovery from blast-induced injury.

Acknowledgments

We thank the Center for Neuroscience and Regenerative Medicine Pre-Clinical Core and NIAAA-FLAC for animal care. We thank Tom Bargar and Nicholas Conoan of the Electron Microscopy Core Facility (EMCF) at the University of Nebraska Medical Center for technical assistance. We also are grateful to Drs. R. Douglas Fields and Dipankar J. Dutta for their expertise in myelin EM methods and all the Holmes laboratory members for valuable discussions and technical advice. We thank Dr. Takashi Kawashima for providing the Matlab code used for the MBP and CNPase intensity analyses. The opinions, interpretations, conclusions, and recommendations are those of the authors and are not necessarily endorsed by the NIH, U.S. Army, Department of Defense, the U.S. Government, or the Uniformed Services University of the Health Sciences.

Authors' Contributions

M.N., O.B., J.T.M., and A.H. designed the experiments. L.B.T., A.H.F., and Y.K. performed the blast procedure. M.N., W.W.T., and L.B.T. collected and analyzed data. M.N., W.W.T., L.B.T., J.T.M., and A.H. wrote the manuscript.

Funding Information

The EMCF is supported by state funds from the Nebraska Research Initiative (NRI) and the University of Nebraska Foundation, and institutionally by the Office of the Vice-Chancellor for Research.

A.H. is supported by the NIAAA Intramural Research Program, and A.H. and J.T.M. are funded by the Henry Jackson Foundation for the Advancement of Military Medicine and the Department of Defense in the Center for Neuroscience and Regenerative Medicine (306136-16.01-6085a5). M.N. is supported by the Uehara Memorial Foundation and Japan Society for Promotion of Science (RPD program).

Author Disclosure Statement

No competing financial interests exist.

References

1. Dewan, M.C., Rattani, A., Gupta, S., Baticulon, R.E., Hung, Y.C., Punchak, M., Agrawal, A., Adeleye, A.O., Shrime, M.G., Rubiano, A.M., Rosenfeld, J.V., and Park, K.B. (2018). Estimating the global incidence of traumatic brain injury. J. Neurosurg. doi: 10.3171/2017.10.JNS17352.
2. G.B.D. Traumatic Brain Injury and Spinal Cord Injury Collaborators. (2019). Global, regional, and national burden of traumatic brain injury and spinal cord injury, 1990–2016: a systematic analysis for the Global Burden of Disease Study 2016. Lancet Neurol. 18, 56–87.
3. Kontos, A.P., Elbin, R.J., Kotwal, R.S., Lutz, R.H., Kane, S., Benson, P.J., Forsten, R.D., and Collins, M.W. (2015). The effects of combat-related mild traumatic brain injury (mTBI): does blast mTBI history matter? J. Trauma Acute Care Surg. 79, 4 Suppl. 2, S146–S151.
4. Mendez, M.F., Owens, E.M., Jimenez, E.E., Peppers, D., and Licht, E.A. (2013). Changes in personality after mild traumatic brain injury from primary blast vs. blunt forces. Brain Inj. 27, 10–18.
5. Mendez, M.F., Owens, E.M., Reza Berenji, G., Peppers, D.C., Liang, L.J., and Licht, E.A. (2013). Mild traumatic brain injury from primary blast vs. blunt forces: post-concussion consequences and functional neuroimaging. NeuroRehabilitation 32, 397–407.
6. Ivanov, I., Fernandez, C., Mitsis, E.M., Dickstein, D.L., Wong, E., Tang, C.Y., Simantov, J., Bang, C., Moshier, E., Sano, M., Elder, G.A., and Hazlett, E.A. (2017). Blast exposure, white matter integrity, and cognitive function in Iraq and Afghanistan combat veterans. Front. Neurol. 8, 127.
7. Lindquist, L.K., Love, H.C., and Elbogen, E.B. (2017). Traumatic brain injury in Iraq and Afghanistan veterans: new results from a national random sample study. J. Neuropsychiatry Clin. Neurosci. 29, 254–259.
8. Kovacs, S.K., Leonessa, F., and Ling, G.S. (2014). Blast TBI models, neuropathology, and implications for seizure risk. Front. Neurol. 5, 47.
9. Katz, E., Ofek, B., Adler, J., Abramowitz, H.B., and Krausz, M.M. (1989). Primary blast injury after a bomb explosion in a civilian bus. Ann. Surg. 209, 484–488.
10. Singh, A.K., Ditkofsky, N.G., York, J.D., Abujudeh, H.H., Avery, L.A., Brunner, J.F., Sodickson, A.D., and Lev, M.H. (2016). Blast injuries: from improvised explosive device blasts to the Boston Marathon bombing. Radiographics 36, 295–307.
11. Xiong, Y., Mahmood, A., and Chopp, M. (2013). Animal models of traumatic brain injury. Nat. Rev. Neurosci. 14, 128–142.
12. Meabon, J.S., Huber, B.R., Cross, D.J., Richards, T.L., Minoshima, S., Pagulayan, K.F., Li, G., Meeker, K.D., Kraemer, B.C., Petrie, E.C., Raskind, M.A., Peskind, E.R., and Cook, D.G. (2016). Repetitive blast exposure in mice and combat veterans causes persistent cerebellar dysfunction. Sci. Transl. Med. 8, 321ra326.
13. Taber, K.H., Warden, D.L., and Hurley, R.A. (2006). Blast-related traumatic brain injury: what is known? J. Neuropsychiatry Clin. Neurosci. 18, 141–145.
14. Fievisohn, E., Bailey, Z., Guettler, A., and VandeVord, P. (2018). Primary blast brain injury mechanisms: current knowledge, limitations, and future directions. J. Biomech. Eng. 140. doi: 10.1115/1.4038710.
15. Vu, P.A., Tucker, L.B., Liu, J., McNamara, E.H., Tran, T., Fu, A.H., Kim, Y., and McCabe, J.T. (2018). Transient disruption of mouse home cage activities and assessment of orexin immunoreactivity following concussive- or blast-induced brain injury. Brain Res. 1700, 138–151.
16. Leonardi, A.D., Bir, C.A., Ritzel, D.V. and VandeVord, P.J. (2011). Intracranial pressure increases during exposure to a shock wave. J Neurotrauma 28, 85–94.
17. Sawyer, T.W., Wang, Y., Ritzel, D.V., Josey, T., Villanueva, M., Shei, Y., Nelson, P., Hennes, G., Weiss, T., Vair, C., Fan, C., and Barnes, J. (2016). High-fidelity simulation of primary blast: direct effects on the head. J. Neurotrauma 33, 1181–1193.
18. Cernak, I. (2015). Blast injuries and blast-induced neurotrauma: overview of pathophysiology and experimental knowledge models and findings, in: *Brain Neurotrauma: Molecular, Neuropsychological, and Rehabilitation Aspects*. E.H. Kobeissy (ed). CRC/Taylor & Francis;: Boca Raton, FL.
19. Long, J.B., Bentley, T.L., Wessner, K.A., Cerone, C., Sweeney, S., and Bauman, R.A. (2009). Blast overpressure in rats: recreating a battlefield injury in the laboratory. J. Neurotrauma 26, 827–840.
20. Koliatsos, V.E., Cernak, I., Xu, L., Song, Y., Savonenko, A., Crain, B.J., Eberhart, C.G., Frangakis, C.E., Melnikova, T., Kim, H., and Lee, D. (2011). A mouse model of blast injury to brain: initial pathological, neuropathological, and behavioral characterization. J. Neuropathol. Exp. Neurol. 70, 399–416.
21. Cernak, I., O'Connor, C. and Vink, R. (2001). Activation of cyclo-oxygenase-2 contributes to motor and cognitive dysfunction following diffuse traumatic brain injury in rats. Clin. Exp. Pharmacol. Physiol. 28, 922–925.
22. Saljo, A., Svensson, B., Mayorga, M., Hamberger, A., and Bolouri, H. (2009). Low-level blasts raise intracranial pressure and impair cognitive function in rats. J. Neurotrauma 26, 1345–1352.
23. Muelbl, M.J., Slaker, M.L., Shah, A.S., Nawarawong, N.N., Gerndt, C.H., Budde, M.D., Stemper, B.D., and Olsen, C.M. (2018). Effects of mild blast traumatic brain injury on cognitive- and addiction-related behaviors. Sci. Rep. 8, 9941.
24. Genovese, R.F., Simmons, L.P., Ahlers, S.T., Maudlin-Jeronimo, E., Dave, J.R., and Boutte, A.M. (2013). Effects of mild TBI from repeated blast overpressure on the expression and extinction of conditioned fear in rats. Neuroscience 254, 120–129.
25. Elder, G.A., Dorr, N.P., De Gasperi, R., Gama Sosa, M.A., Shaughness, M.C., Maudlin-Jeronimo, E., Hall, A.A., McCarron, R.M., and Ahlers, S.T. (2012). Blast exposure induces post-traumatic stress disorder-related traits in a rat model of mild traumatic brain injury. J. Neurotrauma 29, 2564–2575.
26. Perez-Garcia, G., Gama Sosa, M.A., De Gasperi, R., Tschiffely, A.E., McCarron, R.M., Hof, P.R., Gandy, S., Ahlers, S.T., and Elder, G.A. (2019). Blast-induced ''PTSD'': evidence from an animal model. Neuropharmacology 145, 220–229.
27. Belanger, H.G., Kretzmer, T., Yoash-Gantz, R., Pickett, T., and Tupler, L.A. (2009). Cognitive sequelae of blast-related versus other mechanisms of brain trauma. J. Int. Neuropsychol. Soc. 15, 1–8.
28. Schwartz, I., Tuchner, M., Tsenter, J., Shochina, M., Shoshan, Y., Katz-Leurer, M., and Meiner, Z. (2008). Cognitive and functional outcomes of terror victims who suffered from traumatic brain injury. Brain Inj. 22, 255–263.
29. Yurgil, K.A., Barkauskas, D.A., Vasterling, J.J., Nievergelt, C.M., Larson, G.E., Schork, N.J., Litz, B.T., Nash, W.P., and Baker, D.G.; Marine Resiliency Study Team. (2014). Association between traumatic brain injury and risk of posttraumatic stress disorder in active-duty Marines. JAMA Psychiatry 71, 149–157.
30. Wall, P.L. (2012). Posttraumatic stress disorder and traumatic brain injury in current military populations: a critical analysis. J. Am. Psychiatr. Nurses Assoc. 18, 278–298.
31. Schneiderman, A.I., Braver, E.R., and Kang, H.K. (2008). Understanding sequelae of injury mechanisms and mild traumatic brain injury incurred during the conflicts in Iraq and Afghanistan: persistent postconcussive symptoms and posttraumatic stress disorder. Am. J. Epidemiol. 167, 1446–1452.
32. Jorge, R.E., Acion, L., White, T., Tordesillas-Gutierrez, D., Pierson, R., Crespo-Facorro, B., and Magnotta, V.A. (2012). White matter abnormalities in veterans with mild traumatic brain injury. Am. J. Psychiatry 169, 1284–1291.
33. Dennis, E.L., Wilde, E.A., Newsome, M.R., Scheibel, R.S., Troyanskaya, M., Velez, C., Wade, B.S.C., Drennon, A.M., York, G.E., Bigler, E.D., Abildskov, T.J., Taylor, B.A., Jaramillo, C.A., Eapen, B., Belanger, H., Gupta, V., Morey, R., Haswell, C., Levin, H.S., Hinds, S.R., 2nd, Walker, W.C., Thompson, P.M., and Tate, D.F. (2018). Enigma military brain injury: a coordinated meta-analysis of diffusion MRI from multiple cohorts. Proc. IEEE Int. Symp. Biomed. Imaging 2018, 1386–1389.
34. Taber, K.H., Hurley, R.A., Haswell, C.C., Rowland, J.A., Hurt, S.D., Lamar, C.D., and Morey, R.A. (2015). White matter compromise in veterans exposed to primary blast forces. J. Head Trauma Rehabil. 30, E15–E25.
35. Davenport, N.D., Lim, K.O., Armstrong, M.T., and Sponheim, S.R. (2012). Diffuse and spatially variable white matter disruptions are associated with blast-related mild traumatic brain injury. NeuroImage 59, 2017–2024.
36. Yeh, P.H., Guan Koay, C., Wang, B., Morissette, J., Sham, E., Senseney, J., Joy, D., Kubli, A., Yeh, C.H., Eskay, V., Liu, W., French, L.M., Oakes, T.R., Riedy, G., and Ollinger, J. (2017).

Compromised neurocircuitry in chronic blast-related mild traumatic brain injury. Hum. Brain Mapp. 38, 352–369.
37. Miller, D.R., Hayes, J.P., Lafleche, G., Salat, D.H., and Verfaellie, M. (2016). White matter abnormalities are associated with chronic postconcussion symptoms in blast-related mild traumatic brain injury. Hum. Brain Mapp. 37, 220–229.
38. Mac Donald, C.L., Barber, J., Andre, J., Evans, N., Panks, C., Sun, S., Zalewski, K., Elizabeth Sanders, R., and Temkin, N. (2017). 5-Year imaging sequelae of concussive blast injury and relation to early clinical outcome. NeuroImage Clin. 14, 371–378.
39. Ritzel, D.V., Parks, S.A., Roseveare, J., Rude, G., and Sawyer, T.W. (2011). Experimental blast simulation for injury studies. Presented at the RTO Human Factors and Medicine Panel (HFM) Symposium, NATO Science and Technology Organization, Halifax, Nova Scotia, Canada.
40. Jaiswal, S., Knutsen, A.K., Wilson, C.M., Fu, A.H., Tucker, L.B., Kim, Y., Bittner, K.C., Whiting, M.D., McCabe, J.T., and Dardzinski, B.J. (2019). Mild traumatic brain injury induced by primary blast overpressure produces dynamic regional changes in [^{18}F]FDG uptake. Brain Res. 1723, 146400.
41. Bukalo, O., Pinard, C.R., Silverstein, S., Brehm, C., Hartley, N.D., Whittle, N., Colacicco, G., Busch, E., Patel, S., Singewald, N., and Holmes, A. (2015). Prefrontal inputs to the amygdala instruct fear extinction memory formation. Sci. Adv. 1, e1500251.
42. Bukalo, O., Nonaka, M., Weinholtz, C.A., Mendez, A., Taylor, W.W., and Holmes, A. (2021). Effects of optogenetic photoexcitation of infralimbic cortex inputs to the basolateral amygdala on conditioned fear and extinction. Behav. Brain Res. 396, 112913.
43. Gunduz-Cinar, O., Brockway, E., Lederle, L., Wilcox, T., Halladay, L.R., Ding, Y., Oh, H., Busch, E.F., Kaugars, K., Flynn, S., Limoges, A., Bukalo, O., MacPherson, K.P., Masneuf, S., Pinard, C., Sibille, E., Chesler, E.J., and Holmes, A. (2019). Identification of a novel gene regulating amygdala-mediated fear extinction. Mol. Psychiatry 24, 601–612.
44. Brigman, J.L., Wright, T., Talani, G., Prasad-Mulcare, S., Jinde, S., Seabold, G.K., Mathur, P., Davis, M.I., Bock, R., Gustin, R.M., Colbran, R.J., Alvarez, V.A., Nakazawa, K., Delpire, E., Lovinger, D.M., and Holmes, A. (2010). Loss of GluN2B-containing NMDA receptors in CA1 hippocampus and cortex impairs long-term depression, reduces dendritic spine density, and disrupts learning. J. Neurosci. 30, 4590–4600.
45. Feyder, M., Wiedholz, L., Sprengel, R., and Holmes, A. (2007). Impaired associative fear learning in mice with complete loss or haploinsufficiency of AMPA GluR1 receptors. Front. Behav. Neurosci. 1, 4.
46. Kogan, J.H., Frankland, P.W., and Silva, A.J. (2000). Long-term memory underlying hippocampus-dependent social recognition in mice. Hippocampus 10, 47–56.
47. Sanderson, D.J., Good, M.A., Skelton, K., Sprengel, R., Seeburg, P.H., Rawlins, J.N., and Bannerman, D.M. (2009). Enhanced long-term and impaired short-term spatial memory in GluA1 AMPA receptor subunit knockout mice: evidence for a dual-process memory model. Learn. Mem. 16, 379–386.
48. Arancibia-Carcamo, I.L., Ford, M.C., Cossell, L., Ishida, K., Tohyama, K., and Attwell, D. (2017). Node of Ranvier length as a potential regulator of myelinated axon conduction speed. Elife 6, e23329.
49. Franklin, K.B.J., and Paxinos, G. (2001). *The Mouse Brain in Stereotaxic Coordinates*, 2nd ed. Academic: London.
50. Schindelin, J., Arganda-Carreras, I., Frise, E., Kaynig, V., Longair, M., Pietzsch, T., Preibisch, S., Rueden, C., Saalfeld, S., Schmid, B., Tinevez, J.Y., White, D.J., Hartenstein, V., Eliceiri, K., Tomancak, P., and Cardona, A. (2012). Fiji: an open-source platform for biological-image analysis. Nat. Methods 9, 676–682.
51. Baker, W.E. (1973). *Explosions in the Air*. University of Texas Press: Austin, TX.
52. Weiss, C., Lendacki, F.R., Rigby, P.H., Wyrwicz, A.M., Disterhoft, J.F., and Spiess, J. (2020). Conditioned contextual freezing is a neurobehavioral biomarker of axonal injury indicated by reduced fractional anisotropy in a mouse model of blast-induced mild traumatic brain injury. Shock 53, 744–753.
53. Belanger, H.G., Proctor-Weber, Z., Kretzmer, T., Kim, M., French, L.M., and Vanderploeg, R.D. (2011). Symptom complaints following reports of blast versus non-blast mild TBI: does mechanism of injury matter? Clin. Neuropsychol. 25, 702–715.
54. Han, C.J., O'Tuathaigh, C.M., van Trigt, L., Quinn, J.J., Fanselow, M.S., Mongeau, R., Koch, C., and Anderson, D.J. (2003). Trace but not delay fear conditioning requires attention and the anterior cingulate cortex. Proc. Natl. Acad. Sci. U. S. A. 100, 13087–13092.
55. McEchron, M.D., Bouwmeester, H., Tseng, W., Weiss, C., and Disterhoft, J.F. (1998). Hippocampectomy disrupts auditory trace fear conditioning and contextual fear conditioning in the rat. Hippocampus 8, 638–646.
56. Burman, M.A., Simmons, C.A., Hughes, M., and Lei, L. (2014). Developing and validating trace fear conditioning protocols in C57BL/6 mice. J. Neurosci. Methods 222, 111–117.
57. Huerta, P.T., Sun, L.D., Wilson, M.A., and Tonegawa, S. (2000). Formation of temporal memory requires NMDA receptors within CA1 pyramidal neurons. Neuron 25, 473–480.
58. Reger, M.L., Poulos, A.M., Buen, F., Giza, C.C., Hovda, D.A., and Fanselow, M.S. (2012). Concussive brain injury enhances fear learning and excitatory processes in the amygdala. Biol. Psychiatry 71, 335–343.
59. Seo, D.O., Carillo, M.A., Chih-Hsiung Lim, S., Tanaka, K.F., and Drew, M.R. (2015). Adult hippocampal neurogenesis modulates fear learning through associative and nonassociative mechanisms. J. Neurosci. 35, 11330–11345.
60. Bekku, Y., Vargova, L., Goto, Y., Vorisek, I., Dmytrenko, L., Narasaki, M., Ohtsuka, A., Fassler, R., Ninomiya, Y., Sykova, E., and Oohashi, T. (2010). Bral1: its role in diffusion barrier formation and conduction velocity in the CNS. J. Neurosci. 30, 3113–3123.
61. Trapp, B.D., Bernier, L., Andrews, S.B., and Colman, D.R. (1988). Cellular and subcellular distribution of 2′,3′-cyclic nucleotide 3′-phosphodiesterase and its mRNA in the rat central nervous system. J. Neurochem. 51, 859-868.
62. Marinelli, C., Bertalot, T., Zusso, M., Skaper, S.D., and Giusti, P. (2016). Systematic review of pharmacological properties of the oligodendrocyte lineage. Front. Cell. Neurosci. 10, 27.
63. Aggarwal, S., Yurlova, L., Snaidero, N., Reetz, C., Frey, S., Zimmermann, J., Pahler, G., Janshoff, A., Friedrichs, J., Muller, D.J., Goebel, C., and Simons, M. (2011). A size barrier limits protein diffusion at the cell surface to generate lipid-rich myelin-membrane sheets. Dev. Cell 21, 445–456.
64. Caldwell, J.H., Schaller, K.L., Lasher, R.S., Peles, E., and Levinson, S.R. (2000). Sodium channel Na(v)1.6 is localized at nodes of ranvier, dendrites, and synapses. Proc. Natl. Acad. Sci. U. S. A. 97, 5616–5620.
65. Hayes, J.P., Bigler, E.D., and Verfaellie, M. (2016). Traumatic brain injury as a disorder of brain connectivity. J. Int. Neuropsychol. Soc. 22, 120–137.
66. Rosenbluth, J. (1966). Redundant myelin sheaths and other ultrastructural features of the toad cerebellum. J. Cell Biol. 28, 73–93.
67. Mierzwa, A.J., Marion, C.M., Sullivan, G.M., McDaniel, D.P., and Armstrong, R.C. (2015). Components of myelin damage and repair in the progression of white matter pathology after mild traumatic brain injury. J. Neuropathol. Exp. Neurol. 74, 218–232.
68. Sierra-Mercado, D., McAllister, L.M., Lee, C.C., Milad, M.R., Eskandar, E.N., and Whalen, M.J. (2015). Controlled cortical impact before or after fear conditioning does not affect fear extinction in mice. Brain Res. 1606, 133–141.
69. Corne, R., Leconte, C., Ouradou, M., Fassina, V., Zhu, Y., Deou, E., Besson, V., Plotkine, M., Marchand-Leroux, C., and Mongeau, R. (2019). Spontaneous resurgence of conditioned fear weeks after successful extinction in brain injured mice. Prog. Neuropsychopharmacol. Biol. Psychiatry 88, 276–286.
70. Heldt, S.A., Elberger, A.J., Deng, Y., Guley, N.H., Del Mar, N., Rogers, J., Choi, G.W., Ferrell, J., Rex, T.S., Honig, M.G., and Reiner, A. (2014). A novel closed-head model of mild traumatic brain injury caused by primary overpressure blast to the cranium produces sustained emotional deficits in mice. Front. Neurol. 5, 2.
71. Perez Garcia, G., Perez, G.M., De Gasperi, R., Gama Sosa, M.A., Otero-Pagan, A., Pryor, D., Abutarboush, R., Kawoos, U., Hof, P., Cook, D., Gandy, S.E., Ahlers, S., and Elder, G.A. (2021). Progressive cognitive and PTSD-related behavioral traits in rats exposed to repetitive low-level blast. J. Neurotrauma. doi: 10.1089/neu.2020.7398.
72. Perez-Garcia, G., Gama Sosa, M.A., De Gasperi, R., Lashof-Sullivan, M., Maudlin-Jeronimo, E., Stone, J.R., Haghighi, F., Ahlers, S.T., and Elder, G.A. (2018). Chronic post-traumatic stress disorder-related traits in a rat model of low-level blast exposure. Behav. Brain Res. 340, 117–125.

73. Perez-Garcia, G., De Gasperi, R., Gama Sosa, M.A., Perez, G.M., Otero-Pagan, A., Tschiffely, A., McCarron, R.M., Ahlers, S.T., Elder, G.A., and Gandy, S. (2018). PTSD-related behavioral traits in a rat model of blast-induced mTBI are reversed by the mGluR2/3 receptor antagonist BCI-838. eNeuro 5, ENEURO.0357-17.2018.
74. Ratliff, W.A., Mervis, R.F., Citron, B.A., Schwartz, B., Rubovitch, V., Schreiber, S., and Pick, C.G. (2019). Mild blast-related TBI in a mouse model alters amygdalar neurostructure and circuitry. Exp. Neurol. 315, 9–14.
75. Bu, W., Ren, H., Deng, Y., Del Mar, N., Guley, N.M., Moore, B.M., Honig, M.G., and Reiner, A. (2016). Mild traumatic brain injury produces neuron loss that can be rescued by modulating microglial activation using a CB2 receptor inverse agonist. Front. Neurosci. 10, 449.
76. Blaze, J., Choi, I., Wang, Z., Umali, M., Mendelev, N., Tschiffely, A.E., Ahlers, S.T., Elder, G.A., Ge, Y., and Haghighi, F. (2020). Blast-related mild TBI alters anxiety-like behavior and transcriptional signatures in the rat amygdala. Front. Behav. Neurosci. 14, 160.
77. Singewald, N., and Holmes, A. (2019). Rodent models of impaired fear extinction. Psychopharmacology (Berl.) 236, 21–32.
78. Tovote, P., Fadok, J.P., and Luthi, A. (2015). Neuronal circuits for fear and anxiety. Nat. Rev. Neurosci. 16, 317–331.
79. Aravind, A., Ravula, A.R., Chandra, N., and Pfister, B.J. (2020). Behavioral deficits in animal models of blast traumatic brain injury. Front. Neurol. 11, 990.
80. Kaplan, G.B., Leite-Morris, K.A., Wang, L., Rumbika, K.K., Heinrichs, S.C., Zeng, X., Wu, L., Arena, D.T., and Teng, Y.D. (2018). Pathophysiological bases of comorbidity: traumatic brain injury and post-traumatic stress disorder. J. Neurotrauma 35, 210–225.
81. Dutta, D.J., Woo, D.H., Lee, P.R., Pajevic, S., Bukalo, O., Huffman, W.C., Wake, H., Basser, P.J., SheikhBahaei, S., Lazarevic, V., Smith, J.C., and Fields, R.D. (2018). Regulation of myelin structure and conduction velocity by perinodal astrocytes. Proc. Natl. Acad. Sci. U. S. A. 115, 11832–11837.
82. Fields, R.D. (2008). White matter in learning, cognition and psychiatric disorders. Trends Neurosci. 31, 361–370.
83. Auer, F., Vagionitis, S., and Czopka, T. (2018). Evidence for myelin sheath remodeling in the CNS revealed by *in vivo* imaging. Curr. Biol. 28, 549–559.e3.
84. Hildebrand, C., Mustafa, G.Y., and Waxman, S.G. (1986). Remodelling of internodes in regenerated rat sciatic nerve: electron microscopic observations. J. Neurocytol. 15, 681–692.
85. Marion, C.M., Radomski, K.L., Cramer, N.P., Galdzicki, Z., and Armstrong, R.C. (2018). Experimental traumatic brain injury identifies distinct early and late phase axonal conduction deficits of white matter pathophysiology, and reveals intervening recovery. J. Neurosci. 38, 8723–8736.
86. Miyata, S., Taniguchi, M., Koyama, Y., Shimizu, S., Tanaka, T., Yasuno, F., Yamamoto, A., Iida, H., Kudo, T., Katayama, T., and Tohyama, M. (2016). Association between chronic stress-induced structural abnormalities in Ranvier nodes and reduced oligodendrocyte activity in major depression. Sci. Rep. 6, 23084.
87. Barak, B., Zhang, Z., Liu, Y., Nir, A., Trangle, S.S., Ennis, M., Levandowski, K.M., Wang, D., Quast, K., Boulting, G.L., Li, Y., Bayarsaihan, D., He, Z., and Feng, G. (2019). Neuronal deletion of *Gtf2i*, associated with Williams syndrome, causes behavioral and myelin alterations rescuable by a remyelinating drug. Nat. Neurosci. 22, 700–708.
88. Silva, A.I., Haddon, J.E., Ahmed Syed, Y., Trent, S., Lin, T.E., Patel, Y., Carter, J., Haan, N., Honey, R.C., Humby, T., Assaf, Y., Owen, M.J., Linden, D.E.J., Hall, J., and Wilkinson, L.S. (2019). Cyfip1 haploinsufficient rats show white matter changes, myelin thinning, abnormal oligodendrocytes and behavioural inflexibility. Nat. Commun. 10, 3455.
89. Pan, S., Mayoral, S.R., Choi, H.S., Chan, J.R., and Kheirbek, M.A. (2020). Preservation of a remote fear memory requires new myelin formation. Nat. Neurosci. 23, 487–499.
90. Wang, F., Ren, S.Y., Chen, J.F., Liu, K., Li, R.X., Li, Z.F., Hu, B., Niu, J.Q., Xiao, L., Chan, J.R., and Mei, F. (2020). Myelin degeneration and diminished myelin renewal contribute to age-related deficits in memory. Nat. Neurosci. 23, 481–486.
91. Steadman, P.E., Xia, F., Ahmed, M., Mocle, A.J., Penning, A.R.A., Geraghty, A.C., Steenland, H.W., Monje, M., Josselyn, S.A., and Frankland, P.W. (2020). Disruption of oligodendrogenesis impairs memory consolidation in adult mice. Neuron 105, 150–164.e6.
92. Nawarawong, N.N., Slaker, M., Muelbl, M., Shah, A.S., Chiariello, R., Nelson, L.D., Budde, M.D., Stemper, B.D., and Olsen, C.M. (2019). Repeated blast model of mild traumatic brain injury alters oxycodone self-administration and drug seeking. Eur. J. Neurosci. 50, 2101–2112.
93. Bugay, V., Bozdemir, E., Vigil, F.A., Chun, S.H., Holstein, D.M., Elliott, W.R., Sprague, C.J., Cavazos, J.E., Zamora, D.O., Rule, G., Shapiro, M.S., Lechleiter, J.D., and Brenner, R. (2020). A mouse model of repetitive blast traumatic brain injury reveals post-trauma seizures and increased neuronal excitability. J. Neurotrauma 37, 248–261.
94. Calabrese, E., Du, F., Garman, R.H., Johnson, G.A., Riccio, C., Tong, L.C., and Long, J.B. (2014). Diffusion tensor imaging reveals white matter injury in a rat model of repetitive blast-induced traumatic brain injury. J. Neurotrauma 31, 938–950.
95. Badea, A., Kamnaksh, A., Anderson, R.J., Calabrese, E., Long, J.B., and Agoston, D.V. (2018). Repeated mild blast exposure in young adult rats results in dynamic and persistent microstructural changes in the brain. NeuroImage Clin. 18, 60–73.
96. Najm, F.J., Madhavan, M., Zaremba, A., Shick, E., Karl, R.T., Factor, D.C., Miller, T.E., Nevin, Z.S., Kantor, C., Sargent, A., Quick, K.L., Schlatzer, D.M., Tang, H., Papoian, R., Brimacombe, K.R., Shen, M., Boxer, M.B., Jadhav, A., Robinson, A.P., Podojil, J.R., Miller, S.D., Miller, R.H., and Tesar, P.J. (2015). Drug-based modulation of endogenous stem cells promotes functional remyelination in vivo. Nature 522, 216–220.
97. Green, A.J., Gelfand, J.M., Cree, B.A., Bevan, C., Boscardin, W.J., Mei, F., Inman, J., Arnow, S., Devereux, M., Abounasr, A., Nobuta, H., Zhu, A., Friessen, M., Gerona, R., von Budingen, H.C., Henry, R.G., Hauser, S.L., and Chan, J.R. (2017). Clemastine fumarate as a remyelinating therapy for multiple sclerosis (ReBUILD): a randomised, controlled, double-blind, crossover trial. Lancet 390, 2481–2489.
98. Hubler, Z., Allimuthu, D., Bederman, I., Elitt, M.S., Madhavan, M., Allan, K.C., Shick, H.E., Garrison, E., M, T.K., Factor, D.C., Nevin, Z.S., Sax, J.L., Thompson, M.A., Fedorov, Y., Jin, J., Wilson, W.K., Giera, M., Bracher, F., Miller, R.H., Tesar, P.J., and Adams, D.J. (2018). Accumulation of 8,9-unsaturated sterols drives oligodendrocyte formation and remyelination. Nature 560, 372–376.
99. Welliver, R.R., Polanco, J.J., Seidman, R.A., Sinha, A.K., O'Bara, M.A., Khaku, Z.M., Santiago Gonzalez, D.A., Nishiyama, A., Wess, J., Feltri, M.L., Paez, P.M., and Sim, F.J. (2018). Muscarinic receptor M3R signaling prevents efficient remyelination by human and mouse oligodendrocyte progenitor cells. J. Neurosci. 38, 6921–6932.
100. Sangobowale, M., Nikulina, E., and Bergold, P.J. (2018). Minocycline plus N-acetylcysteine protect oligodendrocytes when first dosed 12 hours after closed head injury in mice. Neurosci. Lett. 682, 16–20.

Address correspondence to:
Mio Nonaka, PhD
Laboratory of Behavioral and Genomic Neuroscience
National Institute on Alcohol Abuse and Alcoholism
National Institutes of Health (NIH)
5625 Fishers Lane
Room 2N09
Rockville, MD 20852
USA

E-mail: nonaka@m.u-tokyo.ac.jp